AD-A092 068 ARINC RESEARCH CORP ANNAPOLIS MD F/G 17/5
INFRARED MEASUREMENT VARIABILITY ANALYSIS.(U)
SEP 80 N K MATTHIS, T J MORIN, W E THOMPSON N00173-78-C-0203
UNCLASSIFIED JTCG/AS-79-C-003 NL

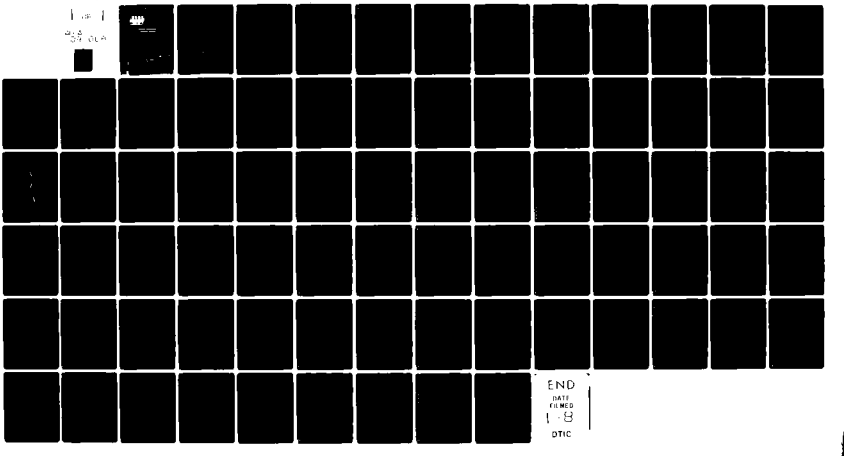

END
DATE FILMED
1-81
DTIC

LEVEL II

AD A092068

INFRARED MEASUREMENT VARIABILITY ANALYSIS

Final Report

R. K. Mueller
T. A. Ellis
R. E. Thompson

September 1980

DTIC
ELECTE
NOV 3 0 1980
S
A

Prepared for

[illegible]

[illegible]

[illegible]

[illegible]

[illegible] were operated by the Naval Weapons Center, China Lake, California, and the Office of Missile Electronic Warfare, White Sands Missile Range, New Mexico.

The contractor was ARINC Research Corporation, Annapolis, Maryland.

Technical direction for this contract was provided by G. [illegible] of the Naval Research Laboratory.

NOTE

[illegible]

[illegible]

UNCLASSIFIED

SECURITY CLASSIFICATION OF THIS PAGE (When Data Entered)

19 REPORT DOCUMENTATION PAGE		READ INSTRUCTIONS BEFORE COMPLETING FORM
1. REPORT NUMBER (18) JTCG/AS-79-C-003	2. GOVT ACCESSION NO. AD-A092068	3. RECIPIENT'S CATALOG NUMBER
4. TITLE (and Subtitle) (6) Infrared Measurement Variability Analysis		5. TYPE OF REPORT & PERIOD COVERED (9) Final rpt. October 1978 - October 1979
		6. PERFORMING ORG. REPORT NUMBER
7. AUTHOR(s) (10) N. K. Matthis, T. J. Morin, W. E. Thompson		8. CONTRACT OR GRANT NUMBER(s) (15) N00173-78-C-0203
9. PERFORMING ORGANIZATION NAME AND ADDRESS ARINC Research Corporation, 2551 Riva Road, Annapolis, MD 21401		10. PROGRAM ELEMENT, PROJECT, TASK AREA & WORK UNIT NUMBERS Project CM 6-05
11. CONTROLLING OFFICE NAME AND ADDRESS (11) JTCG/AS Central Office, AIR-5184J, Naval Air Systems Command, Washington, D.C. 20361		12. REPORT DATE September 1980
		13. NUMBER OF PAGES 68
14. MONITORING AGENCY NAME & ADDRESS (if different from Controlling Office) (12) 77 Naval Research Laboratory, 4555 Overlook Avenue, SW, Washington, D.C. 20375		15. SECURITY CLASS. (of this report) UNCLASSIFIED
		15a. DECLASSIFICATION/DOWNGRADING SCHEDULE

16. DISTRIBUTION STATEMENT (of this Report)

Approved for public release; distribution unlimited; statement applied September 1980.

17. DISTRIBUTION STATEMENT (of the abstract entered in Block 20, if different from Report)

18. SUPPLEMENTARY NOTES

19. KEY WORDS (Continue on reverse side if necessary and identify by block number)

Infrared measurements
Data variability
Interferometers
Measurement uncertainty

20. ABSTRACT (Continue on reverse side if necessary and identify by block number)

See reverse side.

DD FORM 1 JAN 73 1473 EDITION OF 1 NOV 65 IS OBSOLETE
S/N 0102 LF 014 6601

UNCLASSIFIED

SECURITY CLASSIFICATION OF THIS PAGE (When Data Entered)

400247

Naval Research Laboratory

Infrared Measurement Variability Analysis, by N. K. Matthis, T. J. Morin, and W. E. Thompson, ARINC Research Corporation. Washington, D.C., NRL, for Joint Technical Coordinating Group/ Aircraft Survivability. September 1980. 68 pp. (JTCG/AS-79-C-003, publication UNCLASSIFIED.)

Two different Michelson interferometer measurement systems were used to collect spectral radiant intensity data describing blackbody emissions. These data were subjected to statistical and numerical analysis for the purpose of characterizing infrared measurement variability. A mathematical model has been postulated to describe the variability of infrared measurements based on the results of this analysis. Recommendations are made for future study to verify and extend the results presented in this report.

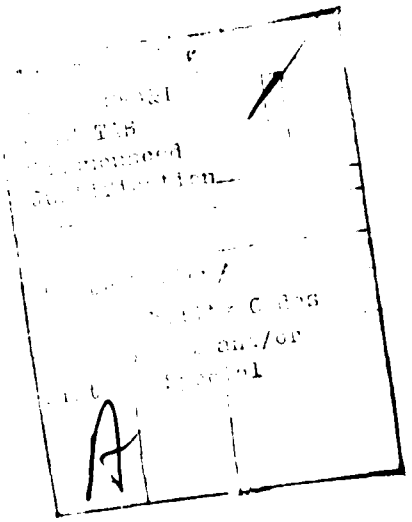

CONTENTS

Figures:

INTRODUCTION

BACKGROUND

The Threat Situation

IR (infrared) guided missiles have been developed to such a degree that they have become a serious threat to aircraft in flight. Detection and tracking systems that rely on the IR emissions of aircraft are an important threat consideration. Newer, more sophisticated IR guidance, detection, and tracking techniques that will very likely increase the threat significantly in the future are being developed.

Every effort is being made to protect friendly aircraft against this threat by controlling and reducing aircraft IR emissions and by improving active countermeasures techniques. Alternatively, the U.S. military community is pursuing the improvement of IR weaponry for defense against enemy aircraft. Therefore, the requirement exists for information on the IR emissions of aircraft.

Needs of the Infrared Community

Several facilities for the measurement of aircraft IR signatures are maintained by various government agencies and by some private companies. However, such measurements are costly and time-consuming. Therefore, the reported results of an aircraft signature measurement program are usually values taken during a one-shot effort in the sense that the aircraft and measurement equipment are positioned one time only for each desired measurement configuration. This leaves unanswered the question of how much difference might occur if data were collected from an attempt to repeat the setup on a different occasion. Likewise, discrepancies occur when several agencies measure one particular orientation of the same aircraft. This can happen even if the various measuring equipments are colocated.

A reported value is customarily an average of several readings taken sequentially with one instrument (radiometer, spectrometer, interferometer). Even the variability of these sequential data samples has not been the subject of a specific study. In short, the costliness of the measurement process has resulted in the fact that no full-scale uncertainty analysis has been performed on the aircraft IR signature measurement process. Data collected by the measurement facilities are reported to the IR community without associated qualifying measurement uncertainty brackets.

Because of the difficulties involved in the direct measurement of aircraft IR signatures, an alternative approach to accumulating descriptive information is being undertaken. This is the calculation of IR emission data by computer programs which model the thermal processes characteristic of operating aircraft. This approach is in a developing state, and there is a need to compare computer outputs with reliable, well-qualified measured data.

An analysis of aircraft IR signature measurement uncertainty would benefit threat designers, developers of suppression and countermeasures techniques, and writers of predictive theoretical computer models, as well as the operators of the measurement facilities.

The Role of JIRS

The JIRS (Joint Infrared Standards) Working Group has been organized to "effect the improvement of the quality of infrared (IR) measurements and their results that pertain to the IR susceptibility of aircraft".* The JIRS Working Group is set up under the Countermeasures Subgroup of JTCG/AS (Joint Technical Coordinating Group on Aircraft Survivability).

In fulfillment of its charter to improve the quality and usability of IR data pertinent to aircraft susceptibility, JIRS has sponsored the measurement variability analysis described in this report. This effort is designed to be integrated into the overall JIRS program of quantifying measurement uncertainty and comparing well-qualified measurement data with computer model aircraft signature predictions.

Scope of This Effort

Aircraft IR signature measurement uncertainty is the result of several factors. A spectrum of possibilities arises from the interplay of all the parameters inherent in the measurement procedures and equipment. In addition, the effects of atmosphere, background, and ambiguity in engine operating conditions must be considered. Finally, the measurement difficulties are severely impacted by the level of error tolerance to which the constantly changing variables associated with in-flight aircraft are measured.

To properly address the problem of quantifying signature measurement uncertainty, all the significant contributors should be isolated and analyzed separately, so that the effect of each can be uniquely determined. The effort described in this report represents one step of the needed total uncertainty study.

The initial phase of a complete signature measurement uncertainty study must consist of quantification of the measurement error factors generic to the measurement equipments and procedures themselves. Several types of measurement devices might be chosen for study including various spectrometers, radiometers, interferometers, and imaging devices. For this beginning effort, the Michelson interferometer was selected.

Three equipments based on similar interferometers are currently in use at three major measurement facilities. These are:

NWC, China Lake, CA	General Dynamics Model No. PFS-101 (w/o optics, software)
OMEW, White Sands, NM	General Dynamics Model No. PFS-201 (w/o software)
General Dynamics, Pomona, CA	General Dynamics Model No. PFS-201

The Michelson interferometers used by the Optical Signatures Branch, Electro-Optics Division of NWC (Naval Weapons Center), China Lake, California, and the Electronic

*Charter for the Joint Infrared Standards Working Group (DRAFT), September, 1978.

Warfare Laboratory, OMEW (Office of Missile Electronic Warfare), White Sands Missile Range, New Mexico, were selected for study. The variability of the measurements taken with these equipments, subject to the procedures routine to their use, is the topic of this report. It is anticipated that subsequent phases of the uncertainty analysis will include aircraft signature data collected by the Pomona Division of General Dynamics Corporation, which is a third major measurement facility using the same type of interferometer.

OBJECTIVES

The goal of this study is to determine quantitatively the variability of data measured with an interferometer system and associated routine procedures, independent of any effects introduced by atmosphere, background, or parameters characteristic of the source of radiation. The factors contributing to the variability discovered will be identified based on a physical understanding of the measurement system and process. Finally, recommendations are listed for analyzing and improving the measurement process and for interpreting data collected from such measurements.

APPROACH

The data base for this study was collected under conditions chosen to minimize the effects of atmosphere, background, and radiation source. A calibrated blackbody source was measured to provide a target that could be theoretically described for later comparison to the measured result. The measurements were made at night to minimize background contributions. Finally, an integrated value of spectral radiant intensity from 3.5 micrometers (μm) to 4.0 μm wavelength was chosen for data analysis to take advantage of the atmospheric window to IR radiation in that wavelength region, thus minimizing atmospheric effects.

Two Michelson interferometer measurement systems, including dedicated computer equipment for performing a Fast Fourier Transform, were used to measure blackbody sources over a variety of source temperatures, source apertures, and distances to target. The possible combinations of these three variables generated a matrix of data cells over three parameters. Whenever sufficient data were available, thirty measurements of integrated spectral radiant intensity from 3.5μm to 4.0μm were obtained for each data cell.

A statistical study of this body of data was performed to determine the data spread within each data cell. Numerical analysis techniques were then applied to try to determine the specific causes of variability.

The Michelson Interferometer

The Michelson interferometer is a rapid-scan, high spectral resolution device which is capable of observing a broad spectrum of IR radiation from an emitting source. The interferogram which results from one scan of the device is converted to a spectral format by the mathematical technique of the Fourier transform, accomplished by dedicated computer equipment which must be considered as part of the measurement system.

To properly determine that contribution to variability which is introduced separately by each of such factors as the width of the "windows" through which the interferogram is digitized by the computer, ambiguity in mathematical approximations internal to the computer process, and so forth, would require an expensive and expert study beyond the scope of the present effort. The total effect of all these factors may by included in the assessment of the variability of an interferometer measurement sample for the purposes of this study.

Summary of Data Collected

Measurement data for this study were collected at facilities operated by NWC and OMEW. The data were reported in graphical and digital form, giving apparent radiant intensity as a function of wavelength. For each graph, the spectral radiant intensity was integrated from 3.5μm to 4.0μm to give a single radiant intensity value for the interval. This integrated value, effective apparent radiant intensity, J, which may be described as

$$J_{\text{eff app}} = \int_{3.5\,\mu\text{m}}^{4.0\,\mu\text{m}} J_\lambda \, d\lambda$$

where J_λ is apparent spectral radiant intensity, was reported by both facilities. For every combination of temperature, aperture, and distance values, thirty samples of this basic data item were obtained whenever possible. The complete data matrix obtained for this effort is listed in Table 1. Figures 1, 2, and 3 show samples of the data supplied by the two measurement facilities.

Both measurement facilities participating in this study customarily report their data as apparent spectral radiant intensity. For most users of the data this is a convenient format, since the physical problem of interest is the IR emission of an aircraft. What any facility actually measures, however, is radiation incident on the collecting optics of the measurement equipment, located at some distance from the source of emission. This irradiance measurement is mathematically converted to radiant intensity by the facility for reporting purposes.

The impact of distance on the variability of IR measurements is an important consideration in the analysis described in this report. Therefore, all the data received from NWC and OMEW were reconverted from radiant intensity to irradiance using the same values for distance as those facilities used for the original conversion. Therefore, the basic data item for this study is

$$H_{3.5\mu\text{m} - 4.0\mu\text{m}} = \int_{3.5\,\mu\text{m}}^{4.0\,\mu\text{m}} H_\lambda \, d\lambda$$

where H_λ is spectral irradiance. There are about thirty samples of this data item in each of the 45 data cells. In addition, each cell corresponds to one measurement each of the three parameters -- temperature, aperture, and distance.

Table 1. List of Measured Data Sets.

Distance, m	Temperature, °K	Aperture, cm^2
Facility: NWC, China Lake		
30.48	805.2	5.067
30.48	805.2	29.200
30.48	805.2	77.070
30.48	805.2	126.700
30.48	994.2	5.067
30.48	993.2	29.200
30.48	990.2	77.070
*30.48	990.2	126.700
30.48	1143.2	5.067
30.48	1143.2	29.200
30.48	1154.7	77.070
30.48	1160.7	126.700
60.96	806.2	5.067
60.96	806.2	29.200
60.96	806.2	72.450
60.96	806.2	101.300
60.96	993.2	5.067
60.96	988.2	29.200
-	-	-
60.96	994.2	101.300
60.96	1140.2	5.067
60.96	1145.7	29.200
-	-	-
*60.96	1141.5	101.300

*Data set has only 27 members.

Table 1. List of Measured Data Sets (Contd.).

Distance, m	Temperature, °F	Aperture, cm^2
-	-	-
-	-	-
152.40	804.4	77.070
152.40	804.7	26.700
152.40	986.2	5.067
152.40	985.7	29.200
152.40	986.2	77.070
-	-	-
152.40	1126.2	5.067
152.40	1142.7	29.200
152.40	1143.2	77.070
152.40	1148.2	126.700
152.40	1148.2	5.067
152.40	1143.2	29.200
152.40	1142.7	77.070
152.40	1126.2	126.700
Facility: OMEW, White Sands		
155	950.26	0.713
155	950.26	5.067
*155	950.26	20.270
155	950.26	45.600
155	1155.86	0.713
155	1155.86	5.067
155	1155.86	20.270
*155	1155.86	45.600
-	-	-
-	-	-
155	1423.76	20.270
155	1423.76	45.600

*Data set has only 29 members.

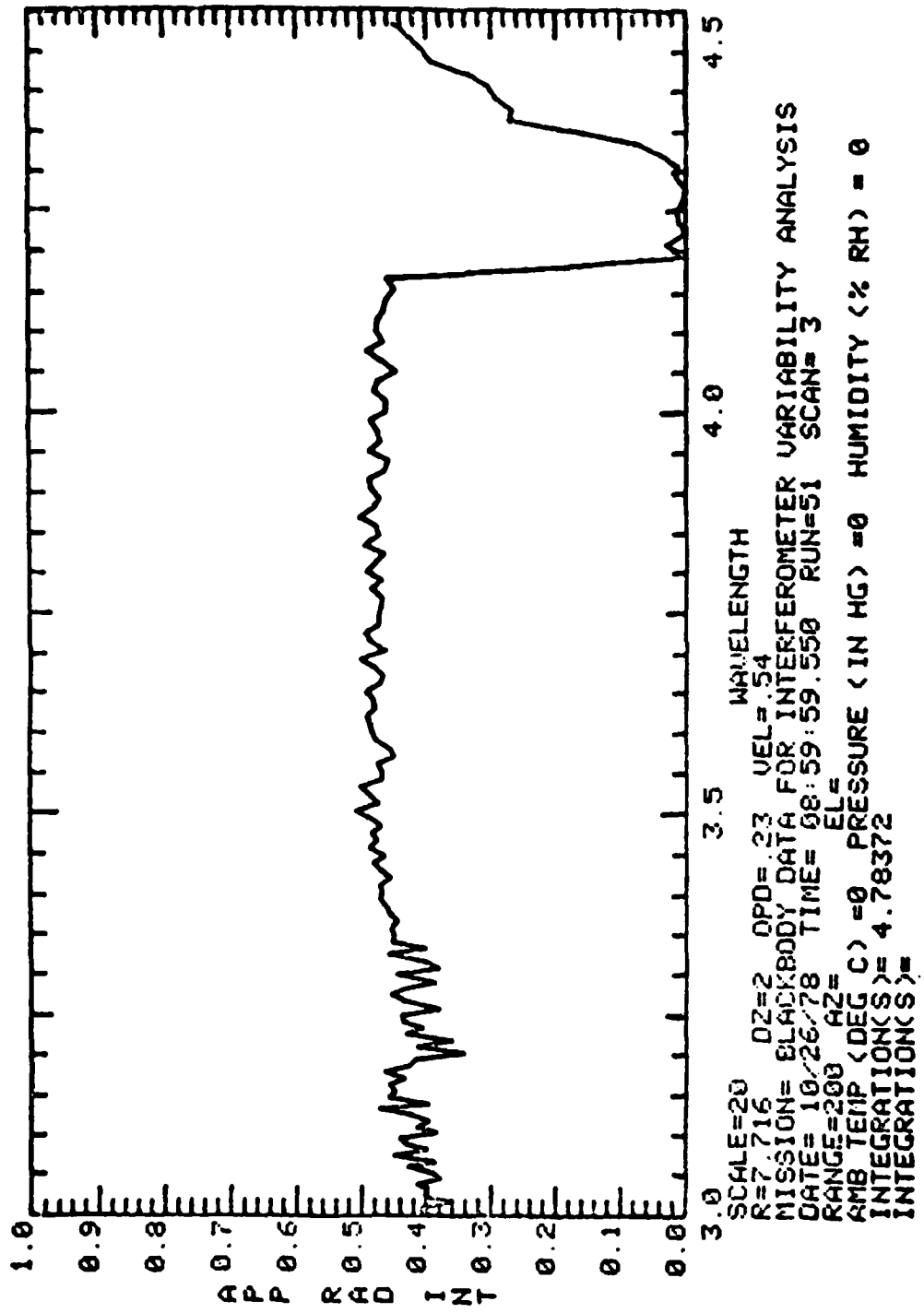

Figure 1. Sample of China Lake Data in Graphical Format.

3.48389	9.46099
3.49328	9.76748
3.50272	10.2451
3.51222	9.5338
3.52176	9.81474
3.53136	10.0853
3.54101	9.43727
3.55071	9.44336
3.56046	9.55742
3.57027	9.06377
3.58013	9.18507
3.59005	9.62242
3.60002	9.7106
3.61005	9.79616
3.62013	9.85863
3.63027	9.66141
3.64047	9.67868
3.65073	9.911
3.66104	9.47626
3.67141	9.40357
3.68184	9.67885
3.69233	10.1045
3.70288	9.32509
3.71349	9.74622
3.72416	9.9205
3.73489	9.51038
3.74569	9.50684
3.75654	9.44898
3.76747	9.3907
3.77845	9.7245
3.7895	9.42853
3.80061	9.8651
3.81179	9.60869
3.82303	9.3728
3.83434	9.9596
3.84572	9.52402
3.85717	9.5976
3.86868	10.0876
3.88026	9.64145
3.89192	9.46629
3.90364	9.74356
3.91543	9.79503
3.9273	9.33596
3.93923	9.20304
3.95124	9.79283
3.96333	9.48575
3.97548	9.54483
3.98772	9.74743
4.00003	9.27392
4.01241	9.3051
4.02487	9.6642
4.03741	9.54128
4.05003	8.99974

Figure 2. Sample of China Lake Data in Digital Format.

DATA> P78A04.08E SCAN>12 KIND>1 M6 NAP2 >3344 ITYPE>2
BG > P78A04.08 SCAN>12 KIND>2 COADD>0 NFFT >8192 NUM >7468
LN2 > SCAN>0 KIND>1 PCTBG>1.00
CAL > P78A01.CB SCAN>5 KIND>3

MEASUREMENT CØNDITIØNS
DATE:17 10 78
TIME:1 :41:32.17

INTEGRATIØN
BANDXX(3.50 -4.00) +0.76051E 00

TARGET CØNDITIØNS
AZ: -108.
EL: -1.
AZ ASPECT ANGLE: 66.30
EL ASPECT ANGLE: 0.02
RANGE: 155.00

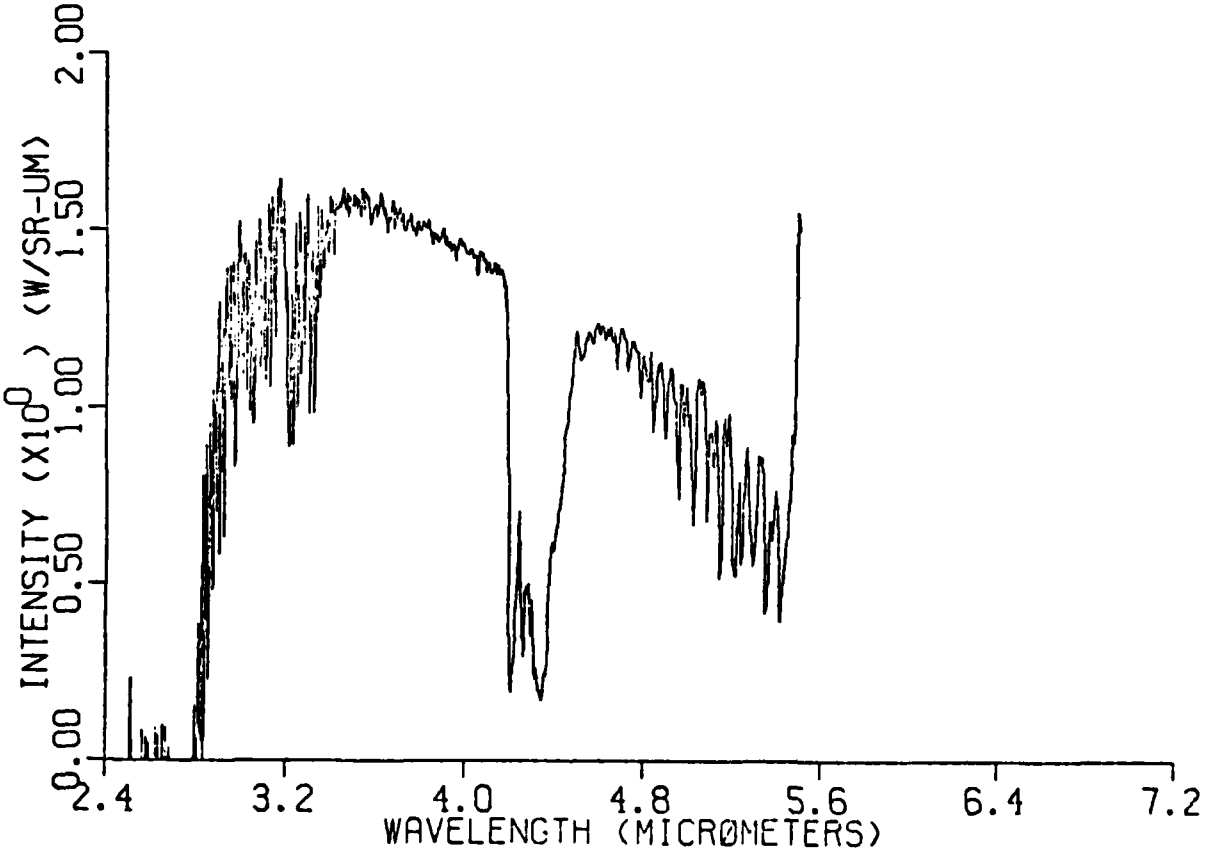

Figure 3. Sample of White Sands Data in Graphical Format.

THE INFRARED MEASUREMENT UNCERTAINTY PROBLEM

THEORY OF MEASUREMENT ERROR

The Meaning of Error

A physical quantity may be assumed to have a unique value*, unknown to man, which scientists attempt to determine as closely as possible by performing experimental measurements. This unique but unknown value is called the *true value*. The value of the physical quantity which is determined by experimental measurement is called the *measured value*. The increment by which the measured value differs from the true value is described as *measurement error*. These concepts are illustrated for a single-valued quantity which can be expressed with a real-number value in Figure 4. Only the measured value of the physical quantity is known. Since the true value is unknown, the magnitude of the measurement error is also unknown. The goal of this section is to discuss all those details which can be learned about the measurement error based on (1) a knowledge about the measurement process, and (2) an examination of the empirical data resulting from the measurement process.

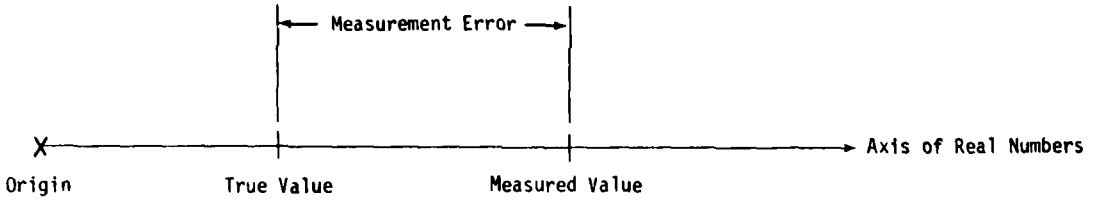

Figure 4. Measurement Error.

Three Kinds of Measurement Error

In general, measurement error is not the result of just one contributing factor. However, all of the measurement error effects which derive from the physical configuration of a measurement system or from the procedures for use of the system can be grouped into three categories. These are:

1. Mistakes, or blunders
2. Constant, or systematic, errors
3. Accidental, or random, errors

The errors in the second category are often called *bias*.

*Excluding the considerations of quantum physics.

As an illustration of these three error categories, consider the case of a man who measures the length of several rods, each of which has a specific function in some equipment. Suppose that he performs the measurements on a warm day by using a steel measuring tape. Due to the increased temperature of the day, the steel tape has expanded from the length it was when the markings were imprinted on it. Also, the tape has a loop on the zero end for convenience in making hand-held measurements. The tape is marked off with centimeters as the smallest scale division.

If the man makes a measurement showing that a rod is 24.3 centimeters in length, and writes down the number 27.3 in his data book due to inattention, this is a blunder. Also, he might make the mistake of recording the correct number, 24.3, but attributing this number in his notes to the wrong rod.

The hasp by which the holding loop is attached to the zero end of the tape may cause the end of the tape always to be improperly aligned with the end of each measured rod, causing all the measurements to be too small by the constant width of the hasp. Also, since the tape has expanded, even if it were properly aligned, all the measurements would suffer the systematic error of being a fraction of what they should be namely, the ratio of the original tape length to the new tape length. If the man, in estimating the distance between the smallest scale divisions marked on the tape, always tends to read low, this will also introduce a systematic error into the measurements.

Finally, there are many measurements which are equally likely to be high or low. The distribution of estimates between smallest scale divisions over and above the personal equation of the man making the measurements is random in nature. So might be the alignment of the zero end of the tape, after the constant effect of the hasp has been accounted for.

The *maximum possible error* which can occur in a measurement excluding blunders is that error which results when the effects of all errors are as additive as possible given the constraints of the measurement process. This would occur in the case of the man measuring rods when:

(1) The hasp is included in the measurement.

(2) The tape is stretched.

(3) The man consistently estimates *low*.

(4) A low reading in the distribution of the man's estimates occurs.

(5) The rod tends to overhang the hasp in this particular instance which has been selected from the distribution of possible alignments.

If all these effects coincide, the maximum error on the low side of true value will be achieved.

The maximum possible error on the low side of true value does not necessarily equal that on the high side. In the example just given, if the personal equation of the man always caused *high* estimates, this would somewhat counteract the other effects. Also, the presence of the hasp will *always* lower the measured value from the true value, whereas the tape may either expand or contract with temperature.

Systematic and random error are shown in Figure 5 as contributing in additive fashion. A probabilistic distribution of random error is indicated in the figure.

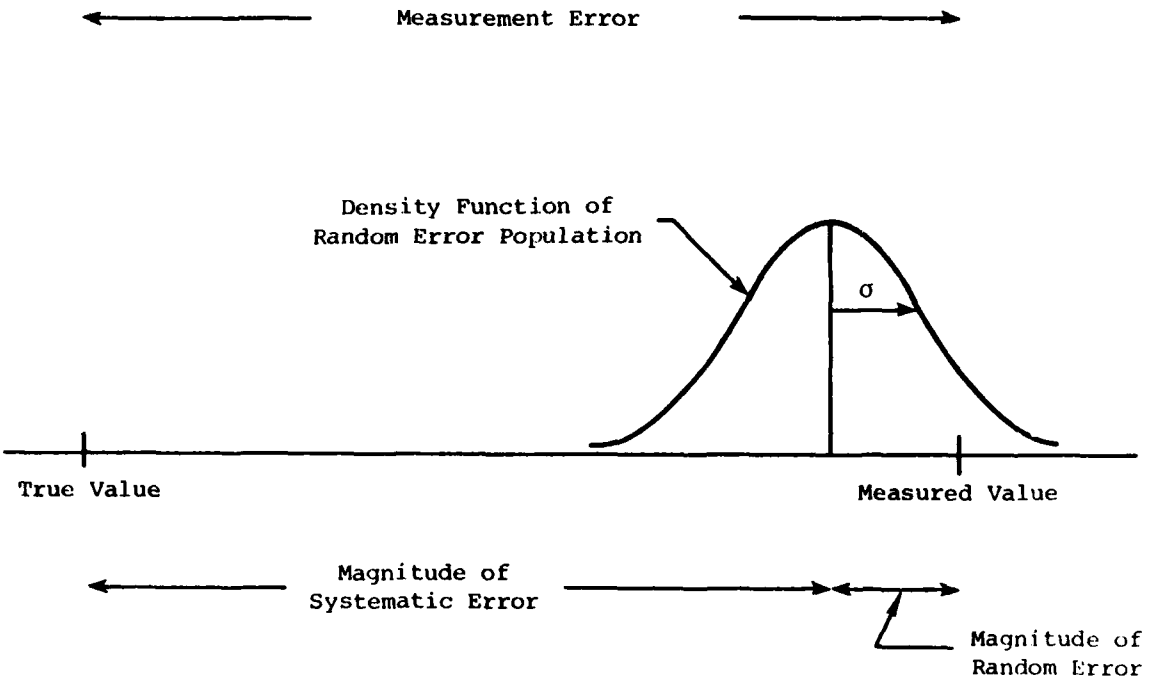

Figure 5. Additive Systematic and Random Error.

Mistakes, or blunders, cannot be predicted. They can be controlled by good procedure and careful attention to detail during data collection. Large mistakes may also be discovered by inspection of the data and eliminated by recomputation of results in some cases.

Systematic errors affect all measurements in the same way. They are usually due to the adjustment or calibration of instrumentation, inherent physical properties of the measurement system, or the personal equations of members of the measurement team. These errors can sometimes be detected by mathematical analysis.

Random errors are usually dealt with in measurement programs by taking several data items and reporting the average value of the sample data set. This method assumes that the probabilistic distribution of random error for the measurement process in question has finite mean and variance.

Inspection of Measurement Data by Graphing

The effects of the three types of measurement error on data can be illustrated graphically as shown in Figure 6. If the true value of a physical quantity could be known, a graph of measured value as a function of true value could be plotted. For perfect measurements this would result in the straight line at 45 degrees inclination shown in the figure. The curve resulting from imperfect measurements is indicated by the dashed line. The dashed line may be displaced from the solid line by a constant amount everywhere along its length (constant error) or it may be displaced by a systematically changing increment (systematic error) or by a combination of these effects.

The data points are indicated by circles. A large blunder can usually be detected by inspection for a continuous function such as the one depicted here. The dotted lines on either side of the dashed line represent the spread of random variation in the data.

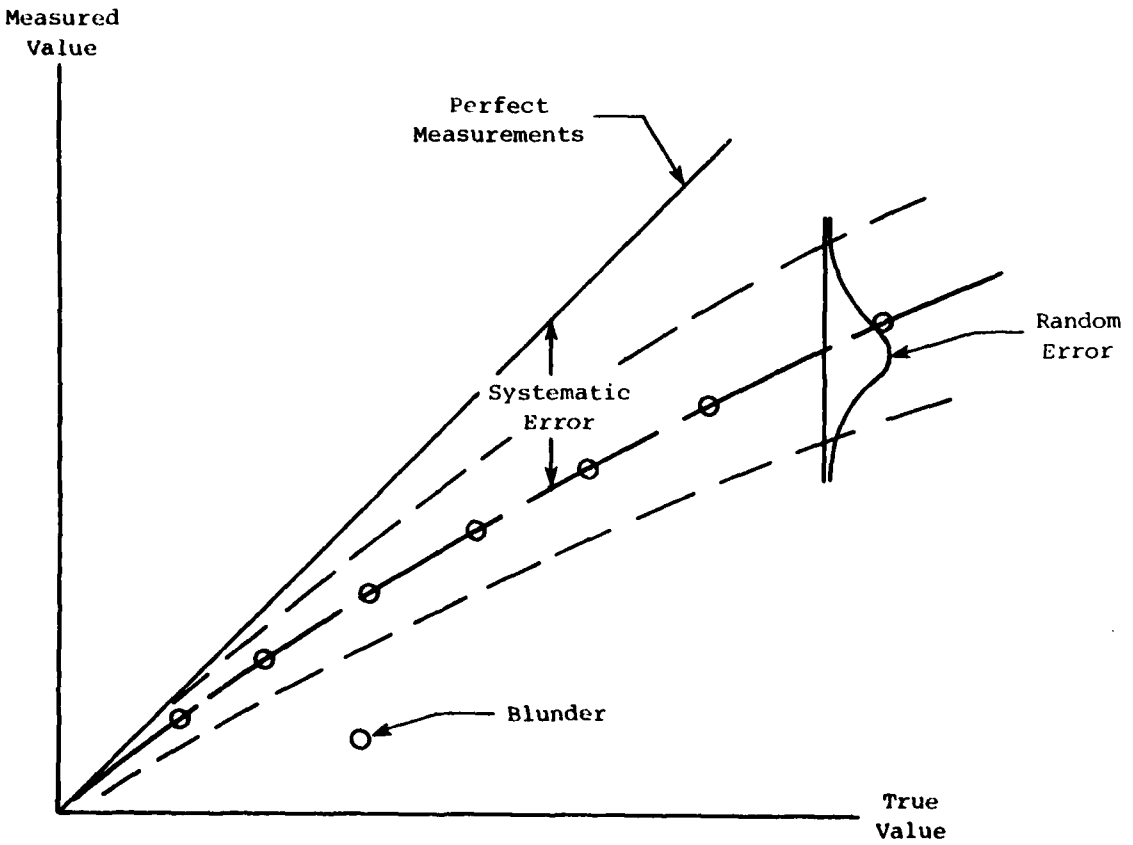

Figure 6. Graphical Inspection of Measurement Data.

This analysis technique can be applied to the data collected for this study if atmospheric effects and system responsivity are included as part of systematic error. The true value of the physical quantity estimated by each data sample is not known. However, Planck's Law can be used to produce a calculated value of integrated spectral irradiance associated with each sample set of data. The comparison of measured irradiance with irradiance values calculated from Planck's Law is discussed in the section of the report entitled *Significant Systematic Differences.*

Precision and Accuracy

The term *precision* describes the repeatability of an experiment, or the success with which the scientist can closely reproduce the same measured value throughout several trials. The spread of the probabilistic distribution of random error is an indication of precision. The magnitude of the displacement of the mean measured value over several trials from the true value relates to *accuracy*, which describes the ability of the scientist to achieve a measured value close to the true value. Precision is improved by reducing the spread of random error; accuracy is improved by decreasing systematic error.

These concepts can be described in terms of the experiment previously examined in which the lengths of several rods were to be measured. If the man were to make some intelligent accounting for the width of the hasp on his measuring tape, the accuracy of his measurements would be improved. If he were to obtain a tape marked off with millimeters as the smallest scale division, his data would be more precise.

Three Ways of Expressing Deterministic Error

Let X represent the true value of a physical quantity.

Let $X + \Delta X$ be the measured value.

Then

$\Delta X = (X + \Delta X) - X$ is called the absolute error

$\Delta X/X$ is called the relative error

$100\ (\Delta X/X)$ is called the percentage error

These are the three most commonly used ways of presenting deterministic estimates of error.

Probabilistic Characterization of Accidental Error

If X is the true value of a physical quantity, then $X_i = (X + \Delta X_i)$ is the measured value of the ith measurement, where ΔX_i is a stochastic component consisting of the sum of the three basic error types:

$$\Delta X_i = \Delta X_{i,\text{blunder}} + \Delta X_{i,\text{systematic}} + \Delta X_{i,\text{random}}$$

If the contributions of blunder have been eliminated by careful inspection of the data, and if the third error term is truly random, with mean zero, then it should be possible to isolate the systematic error term by taking several measurements and averaging them to "zero out" the third term. That is, for N measurements,

$$\frac{\sum_{i=1}^{N} \Delta X_i}{N} = \frac{\sum_{i=1}^{N} \Delta X_{i,\text{systematic}}}{N} + \frac{\sum_{i=1}^{N} \Delta X_{i,\text{random}}}{N}$$

where

$$\frac{\sum_{i=1}^{N} \Delta X_{i,\text{random}}}{N} \rightarrow 0 \text{ as } N \rightarrow \infty$$

For many measurement processes it is reasonable to describe the random component of error ΔX_{random} as having normal (Gaussian) distribution*. The density function of a typical hypothetical infinite population of random error is illustrated in Figure 5. Several characteristics which may be defined for a sample of N data items X_i drawn from such a population are defined in the Appendix, *Statistical Definitions*. These include sample mean and sample standard deviation.

As shown in Figure 5, the sample mean is an indication of systematic error (or accuracy); the standard deviation is descriptive of random error (or precision).

Algebraic Expressions for Error

For any physical quantity which can be expressed as a deterministic function of several measurable parameters, it is possible to describe the exact error in the computed value of that quantity as a function of the exact values of errors in the measured parameters. The following basic rules apply:

For a sum $|A + B|$, the error is

$$|(A + \Delta A) + (B + \Delta B)| - |A + B| = \Delta A + \Delta B$$

For a product $|A \cdot B|$ the error is

$$|(A + \Delta A) \cdot (B + \Delta B)| - |A \cdot B| = B\Delta A + A\Delta B + \Delta A\Delta B$$

For a square $|A^2|$ the error is

$$|(A + \Delta A)^2| - |A^2| = 2A\Delta A + \Delta A^2$$

*The term "normal" for this widely used distribution was introduced by K. Pearson and is the term usually used in applied statistics today. The same distribution has been referred to as the second law of Laplace, the Laplace distribution, the Gauss and the Laplace-Gauss distribution.

Similar considerations apply for all powers, differences, quotients, logarithms, exponentials, etc., but the expressions in some cases are more complex. In the discussion of random errors, where ΔA and ΔB are random variables, the resulting probabilities, together with the possibilities that the true values A and B may be either positive or negative, lead to a tedious computation of distribution functions and proliferation of cases even for sums, products, and squares. The exact analysis relates to the determination of the distribution of products, sums, and more arbitrary functions of possibly dependent random variables. The analysis required in the following does not require this exact procedure for small error analysis (to the order of Δ, ignoring terms of order Δ^2 and higher).

MEASUREMENT UNCERTAINTY

Causes of Measurement Uncertainty for One Measurement System

Whenever a radiating source and an IR measurement system are positioned for the purpose of collecting data describing the source emissions, a unique set of physical conditions prevails at any instant which determines without ambiguity the irradiance at the collecting optics of the instrument. This value is referred to throughout this report as the *true value of irradiance*. Certainly the physical conditions must always include background and atmospheric effects. For a blackbody source, they also include as a minimum the source emissivity, temperature, and aperture, and the separation distance of the source from the measurement system. For a more complex source such as an operating aircraft, many other parameters must be identified, including those describing engine conditions and plume gas dynamics.

If a sample of several measurements is taken corresponding to this unique set of physical conditions, the items in the sample will be probabilistically distributed. A sample mean and variance can be calculated. Then brackets about the sample mean can be specified which can be said with some degree of confidence to contain the true but unknown mean of the infinite population of possible measurements for this unique experimental configuration. If there is no bias in the measurement process and the true value does not change over the measurement period, then the mean of the infinite population of possible measurements will be the true value of the irradiance at the collecting optics. As the sample size drawn from a normally distributed population becomes larger, the brackets about the sample mean which are said to contain the population mean become tighter for any given level of confidence (i.e., the length of the confidence interval decreases inversely as the square root of the sample size). If there is bias in the measurement process, the population mean will be displaced from the true value of irradiance by the amount of the bias.

The probabilistic distribution of individual measurements describes one source of measurement uncertainty. The same equipment measuring the same unique physical conditions will get different results from sample to sample. This concept is illustrated in Figure 7, where μ_H is the population mean and $\bar{H}_1$, $\bar{H}_2$, $\bar{H}_3$, and $\bar{H}_4$ are point estimates of μ_H, or sample means.

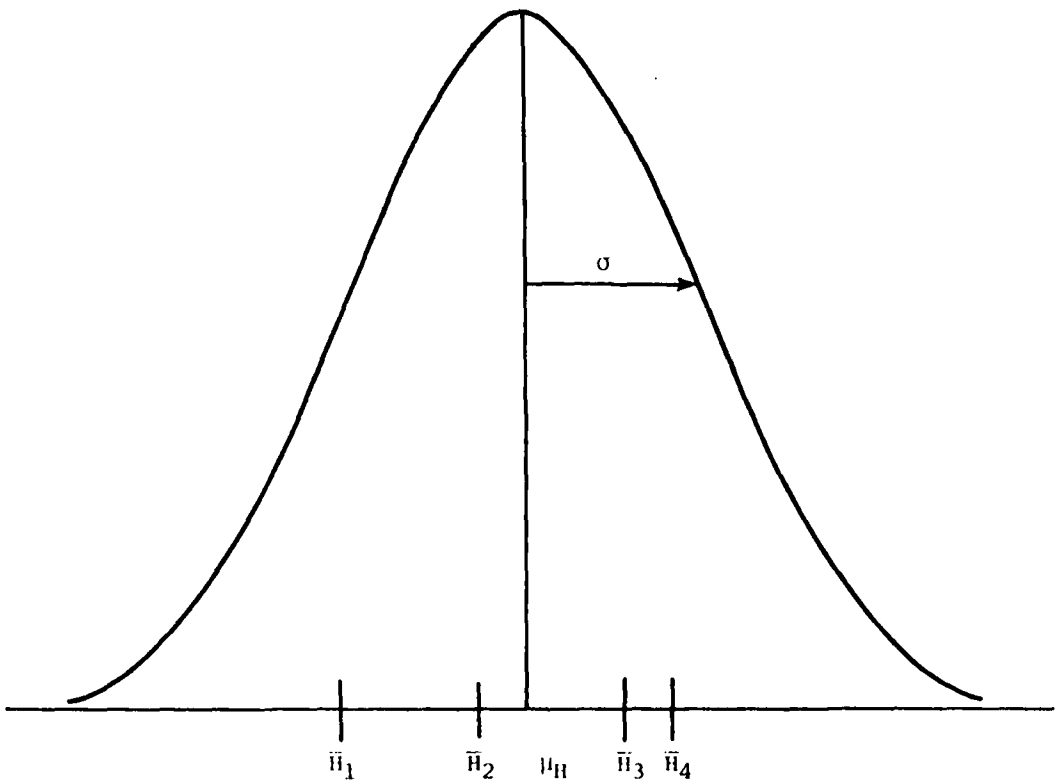

Figure 7. Means of Several Samples Drawn From a Population Having Mean μ_H.

If there is any bias in the measurement process which can change during the course of an experiment, then the same physical conditions measured under two different conditions of bias will yield results that differ by the additive effects of bias, as well as by sample-to-sample variation. An example of this type of bias is the amount by which the system response factor programmed into the measurement process during calibration differs from the true but unknown value of response. This concept of changing bias is illustrated in Figure 8. The true value of response is denoted by R. On the first calibration a value of response $(R + \Delta R_1)$ is measured. On the second calibration a value of response $(R + \Delta R_2)$ is measured. The bias for each measurement sequence is a function of the error in measured response. Within the range of bias variation, the same equipment measuring the same unique physical conditions will get different results from bias condition to bias condition. In fact, all calibrated systems have some bias, since the one-shot system response measurement is itself selected from a probabilistic distribution of possible measured response values.

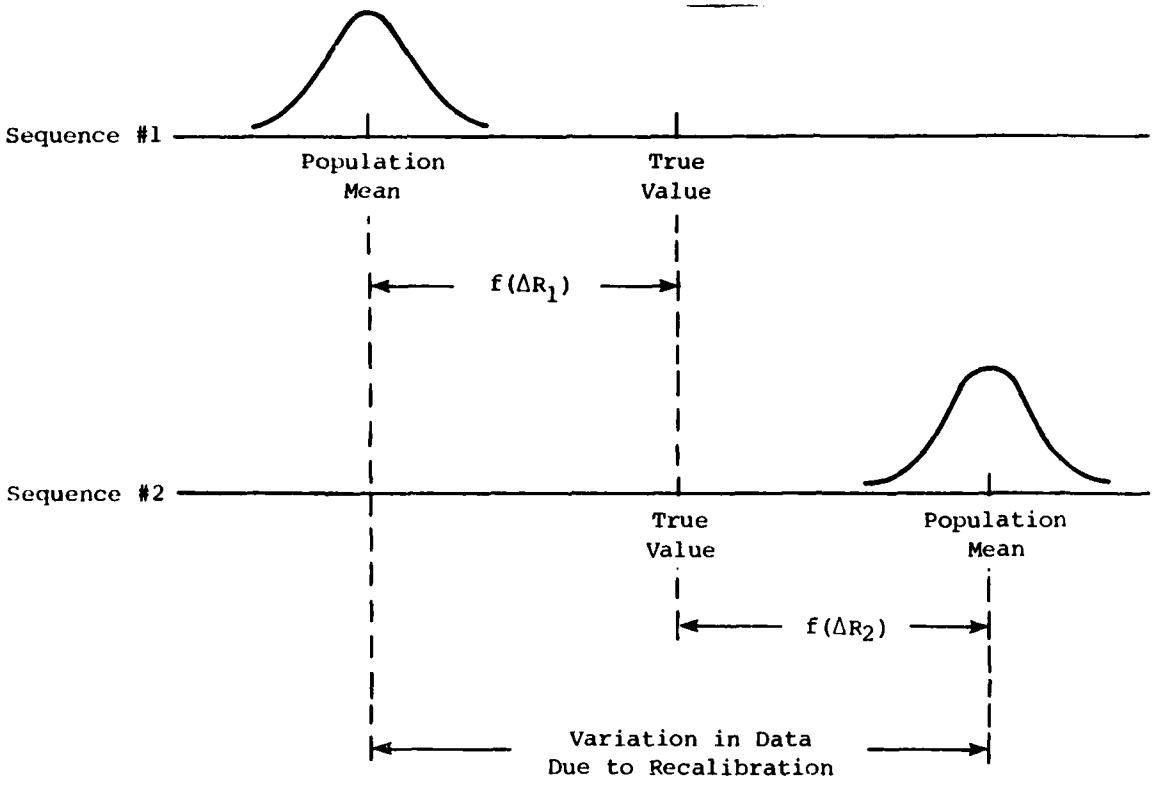

Figure 8. Effect of Changing Bias.

The two causes of data uncertainty just described occur even though a unique set of physical conditions prevails. In addition, there is the problem of reproducing the unique set of physical conditions. Suppose a particular source of IR emissions is measured by a given system on one occasion, and remeasured later by the same system. With what closeness can the background or atmospheric factors be measured in each case? With what accuracy can the same distance to target, the same geometric orientation of the source, the same blackbody temperature or the same engine operating conditions be measured and reproduced? In short, what is the variability in the process of attempting to reproduce the exact same value of irradiance at the collecting optics? This is the third cause of data uncertainty among measurements made by the same system - the reproducibility with which the true value of irradiance for one experiment can be duplicated on a different occasion -- even if that occasion occurs only moments later.

Understanding Uncertainty for One Measurement System

A pictorial representation of the three causes of uncertainty among data describing the same source of emissions and measured by the same equipment is given in Figure 9. The arc BC indicates the range of reproducibility due to human inability to measure accurately the physical conditions, or parameters, which determine a unique experimental configuration. The pointer at the top of the figure is pivoted at a fixed point A, which represents the irradiance at the collecting optics that is assumed to exist. The tip of this pointer may select any value D from the arc BC, where D represents the true irradiance that does in fact exist.

The tip of the first pointer is the pivot point for the second pointer, whose range of variation along the arc EF represents the probabilistic introduction of bias into the measurement process. The point D from which the second pointer is pivoted may lie anywhere along the arc BC, but once its location is determined by a unique experimental configuration, the tip of the second pointer is constrained to vary over an arc EF symmetric about a midpoint directly below D. (This assumes that each bias value is a sample of one drawn from the distribution of possible values for a random bias variable.)

The tip of the second pointer, denoted by G, serves as a pivot for the third pointer at the bottom of the figure. Once a bias value has been determined, by calibration error and perhaps by other system characteristics, the point G is fixed. The tip of the third pointer may travel along arc HJ, symmetric about a midpoint directly below G, where the arc HJ represents sample-to-sample variation in data measured for one unique configuration. The tip of the third pointer K represents the value of irradiance measured by the system.

This representation is not a completely analogous one. The range of the Gaussian, or normal, distribution with which random error has been characterized is infinite; all three arcs are shown as finite in length. Moreover, the points near the center of the arcs have a higher probability of being selected than the points near the ends. However, this figure is useful for visualizing the way in which the three causes of uncertainty in measurement data from the same measurement system may supplement or counteract each other, and how they all contribute to the total uncertainty of the measurement data from an experiment.

The maximum possible error occurs when all three pointers are extended to the left ends of their possible arcs, or when all three pointers are extended to the right ends of their possible arcs. The maximum possible difference between two measurements of the same perceived physical situation made with the same measurement system is represented by the difference between the two maximum possible error configurations just described.

The range of the tip of the second pointer is descriptive of the accuracy of the measurement system. The range of the tip of the third pointer relates to measurement system precision. The first pointer represents the reproducibility of the experiment, or the ability to achieve the same value of irradiance at the collecting optics of the measurement system. It has no relationship to the measurement system.

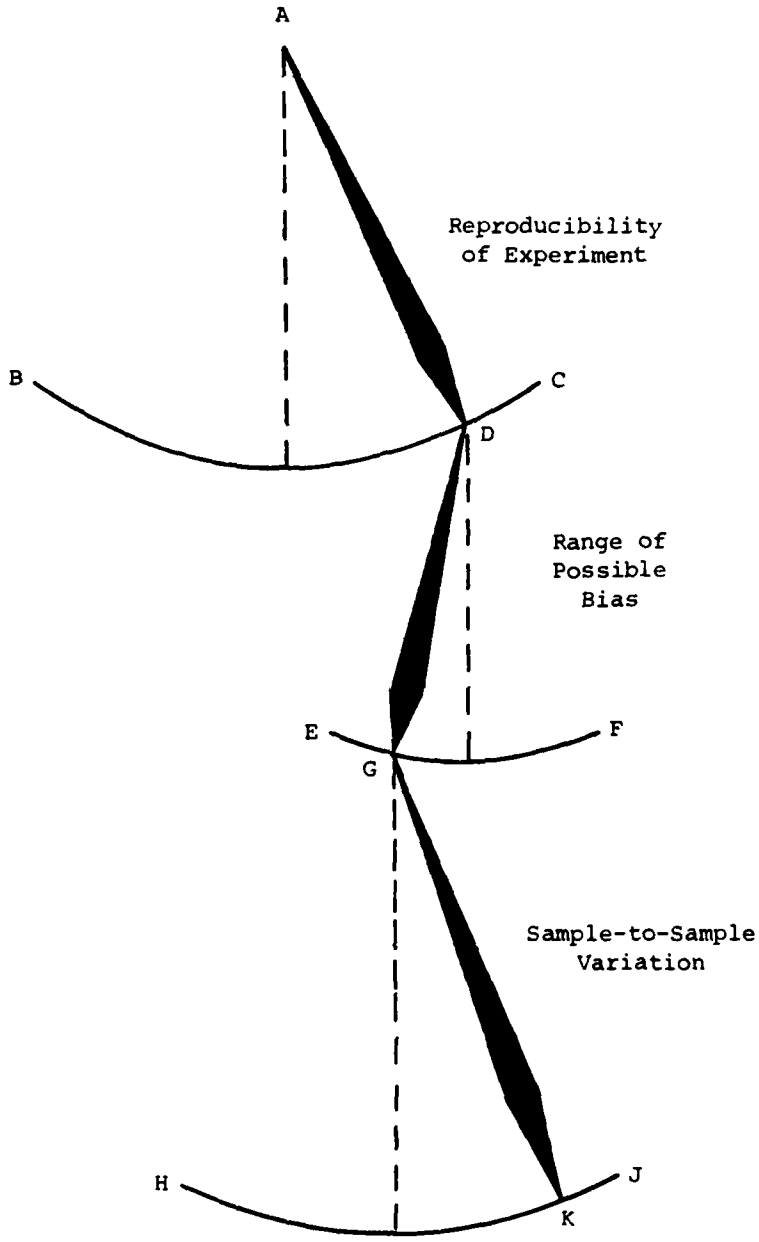

Figure 9. Three Causes of Measurement Uncertainty for *Measurements Made by the Same Equipment.*

The Defining Equations for an Experimental Configuration

An experimental configuration may be described by writing an equation or sequence of equations to define measurement system output as a function of all the physical parameters which determine the configuration. When this is done for the blackbody experiment discussed in this report, the sequence of equations gives (1) irradiance at the collecting optics of the measurement system as a function of the physical parameters which determine the configuration, and (2) system output as a function of irradiance at the collecting optics of the measurement system.

The first equation for the blackbody experiment has the form

$$(1)\quad H_{3.5\,\mu m\ -\ 4.0\,\mu m} = \frac{A\epsilon}{\pi D^2} \int_{3.5\,\mu m}^{4.0\,\mu m} W(\lambda,T) \cdot \tau(\lambda,D)\, d\lambda$$

where

H is the irradiance at the collecting optics of the measurement system

A is the presented area of the aperture of the source of emissions

ϵ is the emissivity of the source

D is the distance from the source to the entrance aperture of the measurement system collecting optics

W is the spectral radiant emittance of the source

τ is the spectral transmittance of the atmosphere

The spectral irradiance at the collecting optics of the measurement system is defined as

$$H(\lambda) = \frac{A\epsilon}{\pi D^2} W(\lambda,T)\tau(\lambda,D)$$

The voltage signal produced by the irradiance at the collecting optics is

$$V(\lambda) = H(\lambda)R(\lambda)$$

where $R(\lambda)$ is the spectral response of the optical system, detector, and system electronics. Finally a transfer function F can be said to operate on the system output $V(\lambda)$, where the operator F represents the dedicated computer processing – including calibration effects, the Fast Fourier Transform, and the integration from 3.5 μm to 4.0 μm. The second equation for the blackbody experiment has the form

$$(2)\quad H_{3.5\,\mu m\ -\ 4.0\,\mu m} = F[H(\lambda) \cdot R(\lambda)]$$

The qualities of accuracy and precision for the experiment relate to the processes described by the second equation. Therefore, the second equation describes that portion of the configuration, namely the measurement system, which introduces the variability represented by the second and third pointers in Figure 9. That is, calibration bias and any other system bias are introduced by the operator F. The very process of measuring -- starting with irradiance $H(\lambda)$ at the collecting optics and ending with values for H printed out from the computer terminal -- introduces sample-to-sample variability.

The reproducibility of the experiment is determined by the first equation. The ambiguity in the true value of irradiance at the collecting optics, given what appear to be successfully reproduced values of the defining parameters, can be expressed in terms of the measurement variances of the defining parameters.

The next three sections of this chapter discuss the analysis of the three causes of data uncertainty for the same source used with the same measurement system.

Quantifying Sample-to-Sample Variability

The variability associated with the probabilistic distribution of measurements, which is a fact of nature that cannot be overcome, can be studied and quantified for any measurement system so that its contribution to the measurement process is understood. Statistical and numerical analysis can be conducted to determine the functional relationship between measurement variance and the magnitude of the measured parameter. This has been attempted for the two systems studied in this report. Several mathematical functions were fitted to the data in an attempt to discover the appropriate formula for

$$\sigma = f(\mu_H, B)$$

where

σ is the standard deviation of the measurement population corresponding to a given set of physical conditions

μ_H is the mean of the measurement population, and, in the absence of bias, is the true value of irradiance at the collecting optics of the measurement system

B is any bias which displaces μ_H from the true value of irradiance

This analysis of the measurement data from China Lake and White Sands is described under *Analysis of the Measured Values.*

Quantifying Reproducibility

The physical parameters which determine an experimental configuration may all be measured when an experiment is performed. If an attempt is made to repeat the experiment, the physical parameters will all be measured a second time, and adjusted until they

seem to have the same values as they did in the first case. (For the blackbody experiment the defining parameters listed were temperature, aperture, distance, emissivity, and atmospheric transmission.) On both the first and second occasions, every last one of these measured parameter values is, by the very nature of things, in error to some extent. On each occasion, the measured value of irradiance is recorded as being the result of all the erroneous values of the physical conditions.

The true value of irradiance H_T at the collecting optics of a measurement system can be expressed algebraically in terms of the defining equation for an experiment. For the blackbody experiment

$$H_T = f(T,A,D,\epsilon,\tau)$$

A *calculated value of irradiance* H_C can be found by inserting the measured parameter values in the defining equation. If ΔT, ΔA, ΔD, $\Delta\epsilon$, and $\Delta\tau$ represent small, random errors in the measured values of the defining parameters for the blackbody experiment, the equation for the calculated value of irradiance has the form

$$H_C = f(T + \Delta T, A + \Delta A, D + \Delta D, \epsilon + \Delta\epsilon, \tau + \Delta\tau)$$

$$= \frac{\partial F}{\partial T}\Delta T + \frac{\partial F}{\partial T}\Delta A + \ldots + O(\Delta^2)$$

For each defining parameter (say T), the measured value (say $T + \Delta T$) is a sample of one drawn from an infinite population of possible measured values. If no bias exists in the process of parameter measurement so that $E(\Delta T) = E(\Delta A) = \ldots = 0$, then the true but unknown mean of the infinite population of possible measured parameter values is the true value of the parameter.* If the measured values of all the parameters are statistically independent, random variables having the true parameter values as their means, the variability of H_C about H_T can be described in terms of the parameter variances. Specifically, for small ΔT, ΔA, and so on, if σ_T, σ_A, σ_D, σ_ϵ, and σ_τ are the standard deviations of the measurement population for T, A, D, ϵ, and τ, then H_C is a random variable about mean $H_T + O(\Delta T^2)$ and

$$\sigma_{H_C}^2 = \left|\frac{\partial F}{\partial T}\right|^2 \sigma_T^2 + \left|\frac{\partial F}{\partial A}\right| \sigma_A^2 + \ldots + O(\Delta^2)$$

If H_T is treated as a constant, then the standard deviation of the difference $(H_C - H_T)$ is exactly the same as the standard deviation of H_C:

$$\sigma_{(H_C - H_T)} = \sigma_{H_C}$$

*This statement ignores considerations relating to the limits of the theoretical and mathematical description of the physical laws involved; i.e., it is assumed that the basic formulas are correct over any range of the parameters involved.

Conversely, this is also the standard deviation of H_T about H_C, which is the concept illustrated by the top pointer in Figure 9. The equation for $\sigma_{(H_C - H_T)}$ is described under *Reproducibility of the Experiment* for the blackbody experiment.

If there is bias in the process of parameter measurement, then the true value of irradiance H_T is not the mean of the distribution of possible calculated values H_C derived from measured parameter values. Instead, the mean of the H_C distribution is displaced from H_T due to the bias. The standard deviation of the H_C distribution, and therefore of the $(H_C - H_T)$ distribution, is unchanged. Therefore the reproducibility of data from the same measurement system is unaffected. (This source of bias must be characterized if comparisons are to be made between two measurement systems.)

Detecting Bias

Any bias which is introduced by the measurement system will be reflected in the measured value of irradiance.* That is, the mean μ_H of the infinite population of possible measurements will not be the direct result H_T of the true values of the defining parameters, but will be the result of those conditions *displaced* by some additional systematic effect. The bias will not affect the calculated value of irradiance. Therefore an examination of the pattern of values of the discrepancy $(\bar{H}_M - H_C)$ may reveal clues about system bias, where $\bar{H}_M$ is the mean of a sample of measurements.

First it must be determined that a significant discrepancy exists. By this is meant a persistent difference between $\bar{H}_M$ and H_C greater than that reasonably expected due to chance alone, where chance deviations are of the order of differences between successive measurement values. This can be done by using a statistical tool called the t-statistic to test the hypothesis that H_C is the mean of the H_M distribution. (This hypothesis is unlikely to be true for the blackbody experiment if only because of the errors ΔT, ΔA, ΔD, $\Delta\epsilon$, and $\Delta\tau$.) If significant discrepancy exists, the patterns of this discrepancy with respect to various milestones in the test run log may be examined. One may ask what the effect of recalibration, breakdown and reconfiguration of equipment, increasing separation of source and measurement system, and so forth is on this pattern of $(\bar{H}_M - H_C)$ values.

While the results of such an examination are not mathematically conclusive, they may point to areas which should be investigated by the measurement team. For instance, suppose all the values of $(\bar{H}_M - H_C)$ were positive following calibration R_1, and all negative following calibration R_2. In spite of the errors ΔT, ΔA, ΔD, $\Delta\epsilon$, $\Delta\tau$, which are not known, this would be a strong indication that the calibration procedure was biasing the measured result. This type of analysis for the blackbody data is presented in the section of this report entitled *Comparison of Measured and Calculated Values.*

*This bias is not to be confused with the bias which may exist in the measurement of the defining parameters, which is a separate problem entirely.

Data Discrepancies Among Different Measurement Systems

When an experiment is performed using one measurement system, and then repeated using a different measurement system, even greater discrepancies may result among the data items than when the same measurement system is used repeatedly. In attempting to reproduce the experiment there are now two variations to be accounted for the variation of calculated irradiance about true irradiance at both facilities and the unexpected differences in true irradiance at the two facilities. If H_{C1} and H_{T1} denote calculated and true irradiance at the first facility, and H_{C2} and H_{T2} denote calculated and true irradiance at the second facility, the reproducibility of the experiment can be defined in terms of the standard deviation of the distribution of the second configuration about the first as

$$\sigma = [\sigma^2(H_{C1} - H_{T1}) + \sigma^2(H_{C2} - H_{T2})]^{1/2}$$

In addition, the bias effects and the sample-to-sample variabilities from both facilities will affect the variability of data items from the experiments.

The application of the concepts of data variability developed in this chapter to the blackbody measurement data collected at China Lake and White Sands is described in the next section of this report. The concepts developed in this chapter are summarized in Table 2.

Convention for Describing Measurement Discrepancies

The terminology used in this report will follow the conventions that

1. *Uncertainty* refers to the interval over which data from one facility can range for the same assumed physical conditions.

2. *Reproducibility* refers to the interval over which data from one facility can range due to human inability to accurately measure all the defining parameters.

3. *Variability* describes the effects introduced by the probabilistic distribution of measurement values for a given measurement system.

Table 2. Summary of Variability Properties of the Experiment for One Measurement System.

Parameter	Accessible data	Measure of variability	Analysis and interpretation
H_C	Defining equation from physical laws (Planck's formula)	Analytical properties of defining equation	Requires knowledge of errors in physical parameters which define the experiment
H_T	None directly accessible	Lack of accuracy in determining physical parameters	Derived by inference from study of H_M, H_C, and $H_M - H_C$
H_M	Repeated measurements under controlled conditions	Root-mean-square deviation from mean value	Using the average value $\bar{H}_M$ from repeated measurements reduces the variability from the random component of measurement error: $\sigma_{\bar{H}_M} = \sigma_{H_M}/\sqrt{N}$
$\bar{H}_M - H_C$	From H_C (defining equation) and $\bar{H}_M$ (repeated measurements)	$\sigma^2 (\bar{H}_M - H_C) = \sigma^2 H_M/\sqrt{N} + \sigma^2 H_C$	Includes bias in $\bar{H}_M$ and errors in H_C
$H_T - H_C$	None directly accessible	Systematic and persistent differences between theory and observation by experimenters for different situations	Analysis of theoretical nature relating to limits of applicability of Planck's formula and to practical measurement and control of defining parameters

ANALYSIS OF EXPERIMENTAL DATA

DATA ACQUISITION

Acquisition Methodology

The goal of the data collection effort was to acquire data representative of the output of the measurement facilities including factors unique to the measurement equipment, the dedicated computer hardware, the particular data reduction computer programs used, and the personal equations of the members of the measurement teams. For this reason, editing of the reduced data was permitted, but only for the purpose of eliminating output which clearly did not correspond to a proper interferometer scan in the opinion of the editors. This same editing process is routinely applied by the facilities to data reported from their regular measurement programs, and is therefore appropriate for this study.

For each temperature/aperture/distance combination, approximately 100 interferometer scans were recorded in analog format on magnetic tape. The distance from the blackbody radiation source to the measurement apparatus was measured with surveyor's tape. The interferograms were translated to spectral irradiance by the dedicated computer equipment. The measured distance was used to compute spectral radiant intensity on the computer. The computer output consisted of both digital and graphical representations of spectral radiant intensity (see Figures 1, 2, and 3).

Except for cases where editing removed an output graph from the sequence of scans, 30 sequentially numbered scans were used. For the two facilities, these were designated as:

China Lake	Scans 3-32
White Sands	Scans 10-39

This arbitrary selection was chosen to preclude the judicious choice of the "best" 30 out of 100 scans by a facility to improve the apparent variability of reported data. Substitutions for edited scans were required to be made in sequence following the last scan requested until a sample of 30 scans was reported.* The integrated value of spectral radiant intensity from 3.5μm to 4.0μm was calculated during the computer processing and reported for each scan.

China Lake Equipment Configuration

The radiation source used in the China Lake portion of the experiment was a blackbody with a 1/2-inch diameter cavity. This source was positioned at the focal point of the optics of a parabolic reflector of 25-inch focal length with a 5-inch diameter mirror. Four stops were placed across the collimated beam of radiation to provide a range of aperture sizes. A range of three nominal temperatures was covered. The source was observed with a General Dynamics Model PFS-101 Michelson interferometer from distances of 100, 200, and 500 feet. The measurement system field-of-view was 4.5 degrees.

*Some of the data sets were delivered with fewer than 30 members. These data sets were included in the study as received, due to the costs associated with acquiring the additional requested scans.

White Sands Equipment Configuration

The data collection effort performed by OMEW was conducted at Mar Site on the Army White Sands Missile Range, New Mexico. The IR radiation source used was a blackbody with a 3-inch diameter aperture. Apertures of varying size were placed in front of the blackbody aperture to provide the range of values for that parameter. The blackbody temperature was thermostatically controlled. The reported temperature was recorded from a digital readout to one decimal place associated with a temperature probe inserted in the cavity of the blackbody distinct from the temperature probe associated with the thermostatic control. The source was observed with a General Dynamics Model PFS-201 Michelson interferometer located at a distance of 500 feet from the blackbody. The collecting optics of the interferometer had a field-of-view of 0.6 degrees.

ANALYSIS OF THE MEASURED VALUES

Statistical Analysis

Some basic characteristics of the measured data samples have been developed in accordance with the formulas presented in the Appendix to this report. These values are listed for the China Lake data in Table 3 and for the White Sands data in Table 4. For each data sample, a calculated value of irradiance is given, derived from application of Planck's Law to the measured values of temperature, aperture, and distance for the data cell. The mean of each data sample is given as the *measured value of irradiance*. The *standard deviation* is descriptive of the spread of the sample about the mean.

Tests for Normalcy

One way of determining whether a normal distribution represents a good fit for given data is to use probability (Gaussian) graph paper. The percentage cumulative frequency of the data sample is plotted as a function of the measured parameter. The degree to which all the plotted points lie on a straight line determines the closeness of fit of the given distribution to a normal distribution. This method has been used to determine the normalcy of the irradiance data samples by inspection. A sample plot is shown in Figure 10.

Analysis of Skewness and Kurtosis

Skewness describes the degree to which a distribution departs from a symmetric configuration. The *moment coefficient of skewness*, defined as the third moment about the mean divided by the cube of the standard deviation (see Appendix), has a value of zero for perfectly symmetrical curves such as the normal curve. If the computed skewness of a distribution is positive, the distribution has a longer "tail" to the right of the maximum of the curve. If the skewness is negative, there is a longer "tail" to the left of the maximum.

Table 3. Characteristics of the China Lake Data Samples.

Distance, m	Temperature, °K	Aperture, cm^2	Calculated value of irradiance	Mean measured value of irradiance	Standard deviation of sample
152.40	804.4	77.07	2.27 E-08	2.24 E-08	7.06 E-10
	804.7	126.7	3.74 E-08	3.60 E-08	8.43 E-10
	986.2	5.067	3.65 E-09	2.65 E-09	3.25 E-10
	985.7	29.2	2.10 E-08	1.71 E-08	6.55 E-10
	986.2	77.07	5.55 E-08	4.73 E-08	9.90 E-10
	1126.2	5.067	6.01 E-09	5.39 E-09	3.58 E-10
	1142.7	29.2	3.64 E-08	3.35 E-08	7.85 E-10
	1143.2	77.07	9.63 E-08	8.98 E-08	2.37 E-09
	1148.2	126.7	1.61 E-07	1.46 E-07	2.26 E-09
	1126.2	5.067	6.01 E-09	5.67 E-09	4.29 E-10
	1142.7	29.2	3.64 E-08	3.56 E-08	7.21 E-10
	1143.2	77.07	9.63 E-08	9.52 E-08	2.51 E-09
	1148.2	126.7	1.61 E-07	1.55 E-07	2.53 E-09
60.96	806.2	5.067	9.44 E-09	9.45 E-09	7.19 E-10
	806.2	29.2	5.44 E-08	5.29 E-08	8.78 E-10
	806.2	72.45	1.35 E-07	1.26 E-07	1.52 E-09
	806.2	101.3	1.89 E-07	1.76 E-07	1.98 E-09
	993.2	5.067	2.35 E-08	2.34 E-08	6.09 E-10
	988.2	29.2	1.33 E-07	1.30 E-07	1.36 E-09
	994.2	101.3	4.71 E-07	4.47 E-07	3.12 E-09
	1140.2	5.067	3.92 E-08	4.11 E-08	1.01 E-09
	1145.7	29.2	2.30 E-07	2.28 E-07	2.33 E-09
	1141.5	101.3	7.87 E-07	7.77 E-07	9.91 E-09
30.48	805.2	5.067	3.75 E-08	3.76 E-08	1.43 E-09
	805.2	29.2	2.16 E-07	2.16 E-07	1.67 E-09
	805.2	77.07	5.71 E-07	5.84 E-07	2.89 E-09
	805.2	126.7	9.38 E-07	8.34 E-07	2.94 E-09
	994.2	5.067	9.42 E-08	9.65 E-08	1.22 E-09
	993.2	29.2	5.41 E-07	5.39 E-07	3.49 E-09
	990.2	77.07	1.41 E-06	1.44 E-06	3.97 E-09
	990.2	126.7	2.32 E-06	2.09 E-06	6.43 E-09
30.48	1143.2	5.067	1.58 E-07	1.69 E-07	1.30 E-09
	1143.2	29.2	9.12 E-07	9.11 E-07	3.14 E-09
	1154.7	77.07	2.49 E-06	2.57 E-06	7.87 E-09
	1160.7	126.7	4.17 E-06	3.79 E-06	8.91 E-09

Table 4. Characteristics of the White Sands Data Samples.

Distance, m	Temperature, °K	Aperture, cm^2	Calculated value of irradiance	Mean measured value of irradiance	Standard deviation of sample
155.0	950.26	0.713	4.27 E-10	4.45 E-10	1.77 E-11
	950.26	5.067	3.04 E-09	3.18 E-09	3.81 E-11
	950.26	20.27	1.21 E-08	1.24 E-08	9.09 E-11
	950.26	45.6	2.73 E-08	2.75 E-08	8.92 E-11
	1155.86	0.713	8.94 E-10	9.18 E-10	1.72 E-11
	1155.86	5.067	6.36 E-09	6.43 E-09	7.20 E-11
	1155.86	20.27	2.54 E-08	2.57 E-08	2.73 E-10
	1155.86	45.6	5.72 E-08	5.72 E-08	3.43 E-10
	1423.76	20.27	4.92 E-08	4.87 E-08	3.51 E-10
	1423.76	45.6	1.11 E-07	1.15 E-07	8.10 E-10

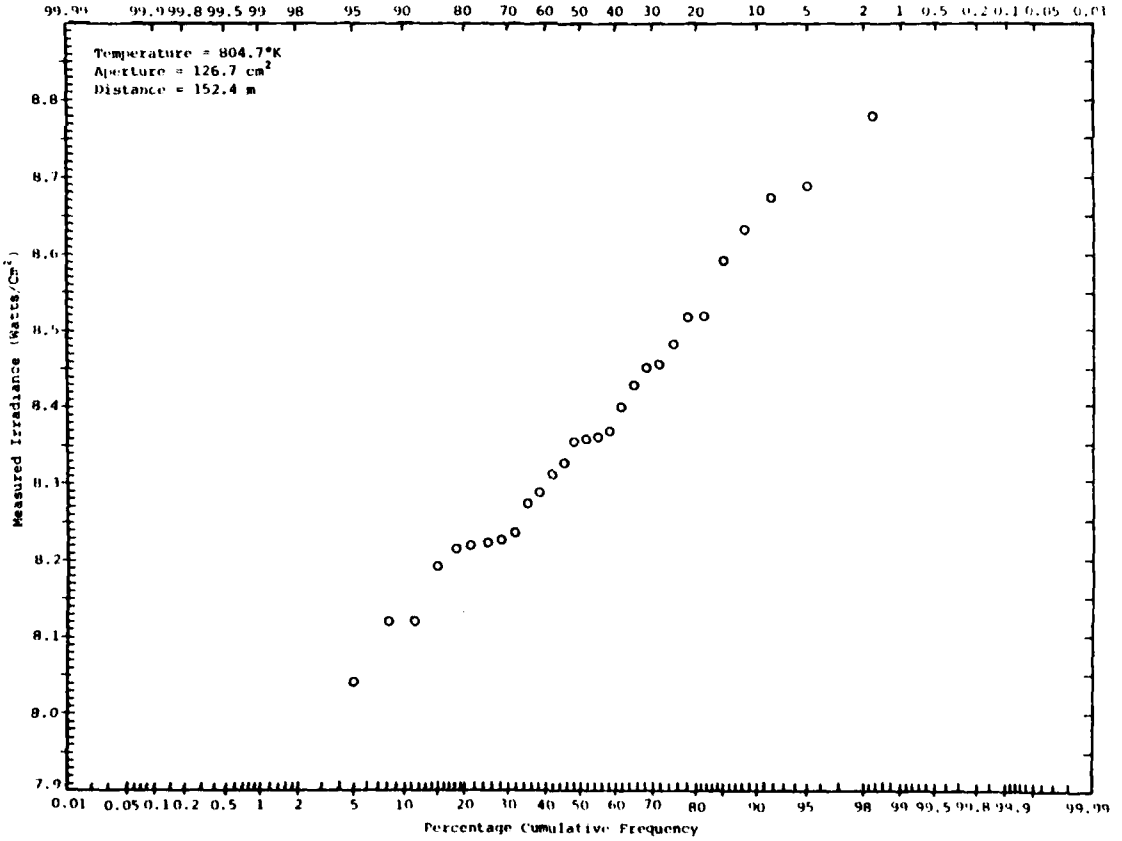

Figure 10. Test of Normalcy for China Lake Irradiance Measurements.

Kurtosis describes the "peakedness" of a distribution. The *moment coefficient of kurtosis*, defined as the fourth moment about the mean divided by the fourth power of the standard deviation (see Appendix), has a value of three for the normal curve. The normal curve is described as moderately peaked, or *mesokurtic*. For values greater than three, a distribution becomes more peaked, or *leptokurtic*. For values less than three, a distribution is flatter, or *platykurtic*. The concepts of skewness and kurtosis are illustrated in Figure 11.

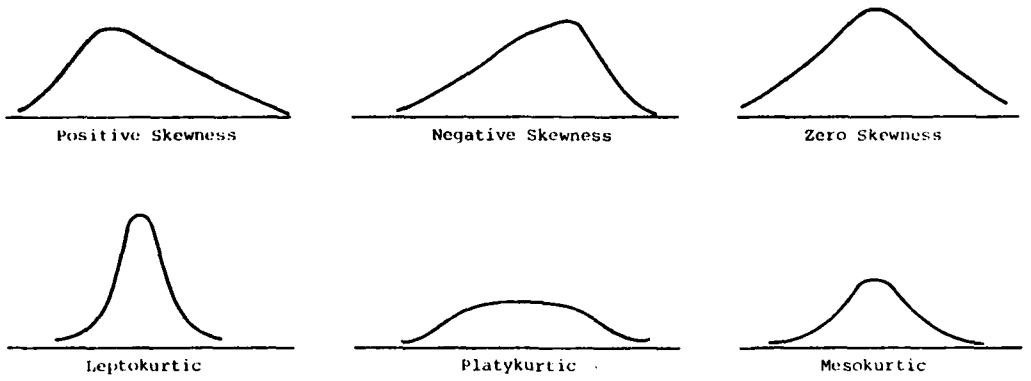

Figure 11. Skewness and Kurtosis.

For a data sample of size N, unbiased estimates of the moment coefficient of skewness, g_1, and the excess of the kurtosis over that of the normal curve, g_2, may be computed.*

It can be shown that if all possible samples of size N were drawn, all the estimates of g_1 would be distributed with a standard deviation of

$$S_{g_1} \simeq (6/N)^{1/2}$$

and all the estimates of g_2 would be distributed with a standard deviation of

$$S_{g_2} \simeq (24/N)^{1/2}$$

These facts have been used to test the irradiance data samples analytically for normalcy. Unbiased estimates of skewness and excess have been developed for all the data samples. These estimates have been compared with the standard deviations for their distributions. All data samples having estimates of skewness and excess within three standard deviations of the values for the normal curve will be described as well-fitted by a normal distribution.

The estimates of skewness and excess for the data samples are given in Table 5 for China Lake and Table 6 for White Sands. Also given are the numbers of standard deviations by which these estimates exceed those for the normal distribution.

*See Mathematics of Statistics, Part Two, by J. F. Kenney and E. S. Keeping, Van Nostrand, 1951, pp. 109-110.

Table 5. Unbiased Estimates of the Skewness and Excess for China Lake Data Samples.

Distance, m	Temperature, °K	Aperture, cm^2	Estimate of skewness	Skewness in standard deviations	Estimate of excess	Excess in standard deviations
152.40	804.4	77.07	-0.575	-1.287	-0.219	-0.245
	804.7	126.7	0.080	0.179	-0.002	-0.002
	986.2	5.067	0.867	1.938	0.193	0.216
	985.7	29.2	0.308	0.690	-0.337	-0.377
	986.2	77.07	-0.356	-0.797	-0.536	-0.599
	1126.2	5.067	0.074	0.165	-0.846	-0.946
	1142.7	29.2	-0.200	-0.447	1.002	1.120
	1143.2	77.07	-1.203	-2.690	2.630	2.941
	1148.2	126.7	-0.247	-0.553	0.391	0.437
	1126.2	5.067	-0.182	-0.407	-0.493	-0.552
	1142.7	29.2	0.408	0.912	0.254	0.284
	1143.2	77.07	-1.078	-2.411	2.384	2.666
	1148.2	126.7	-0.031	-0.069	-0.172	-0.192
60.96	806.2	5.067	0.360	0.805	-0.513	-0.574
	806.2	29.2	-0.074	-0.166	-1.051	-1.175
	806.2	72.45	-0.315	-0.704	-0.488	-0.545
	806.2	101.3	0.476	1.064	0.495	0.554
	993.2	5.067	0.070	0.157	-0.899	-1.005
	988.2	29.2	0.260	0.581	0.136	0.152
	994.2	101.3	0.151	0.339	-0.604	-0.675
	1140.2	5.067	-0.211	-0.471	-0.460	-0.515
	1145.7	29.2	0.182	0.408	-1.122	-1.255
	1141.5	101.3	1.096	2.325	1.727	1.832
30.48	805.2	5.067	-0.251	-0.562	-0.901	-1.007
	805.2	29.2	-0.235	-0.525	-0.726	-0.812
	805.2	77.07	-0.115	-0.258	0.313	0.350
	805.2	126.7	0.205	0.459	-0.587	-0.657
	994.2	5.067	0.357	0.799	0.431	0.482
	993.2	29.2	-0.343	-0.766	0.485	0.542
	990.2	77.07	-0.444	-0.994	-0.616	-0.689
	990.2	126.7	-0.361	-0.766	-0.241	-0.255
	1143.2	5.067	-0.268	-0.599	-0.651	-0.728
	1143.2	29.2	0.186	0.417	-0.459	-0.513
	1154.7	77.07	-0.711	-1.589	0.440	0.492
	1160.7	126.7	0.198	0.443	-1.004	-1.122

Table 6. Unbiased Estimates of the Skewness and Excess for White Sands Data Samples.

Distance, m	Temperature, °K	Aperture, cm^2	Estimate of skewness	Skewness in standard deviations	Estimate of excess	Excess in standard deviations
155.0	950.26	0.713	0.221	0.493	-0.685	-0.766
	950.26	5.067	0.235	0.526	-0.495	-0.553
	950.26	20.27	0.480	1.055	-0.264	-0.290
	950.26	45.6	0.677	1.514	-0.022	-0.025
	1155.86	0.713	0.715	1.599	0.580	0.649
	1155.86	5.067	-0.299	-0.669	0.462	0.517
	1155.86	20.27	-0.631	-1.410	0.995	1.112
	1155.86	45.6	0.401	0.882	1.049	1.154
	1423.76	20.27	-0.002	-0.004	-0.331	-0.370
	1423.76	45.6	0.976	2.181	1.596	1.785

Kolmogorov-Smirnov Test for Normalcy

In the two preceding sections, methods of data inspection were described which enable an analyst to determine whether a normal distribution is a reasonable description of measurement data. To give credibility to the assumption, however, an analytical test for goodness of fit between the measurement data and a particular normal curve should be applied. The Kolmogorov-Smirnov test is just such an analytical procedure for testing goodness of fit between empirical data and a specified theoretical distribution.

In order to apply this method as a test for normalcy, a theoretical normal curve must be specified. This is done by using the sample mean and sample standard deviation as point estimates of the population characteristics. The numerical sample values for mean and standard deviation are used in place of μ and σ, respectively, in the equation for the normal density function

$$Y = \frac{1}{\sigma\sqrt{2\pi}} \exp\left[\frac{-(x-\mu)^2}{2\sigma^2}\right]$$

The normal ogive curve for the specified equation is plotted. Dashed curves are plotted above and below the ogive corresponding to some preselected level of significance to create a "decision band" within which the specified equation is accepted. (A significance level of α implies that 100 α% of the time this test will reject the curve fit when it is an appropriate one.) The measurement data are plotted on the same graph, and if all the data points lie within the decision band, the normal curve fit is accepted. Figure 12 is an illustration of the Kolmogorov-Smirnov test applied to one of the China Lake data samples. This sample had the largest moment coefficient of skewness and excess of kurtosis. All the data points lie within the decision band and the assumption is accepted.

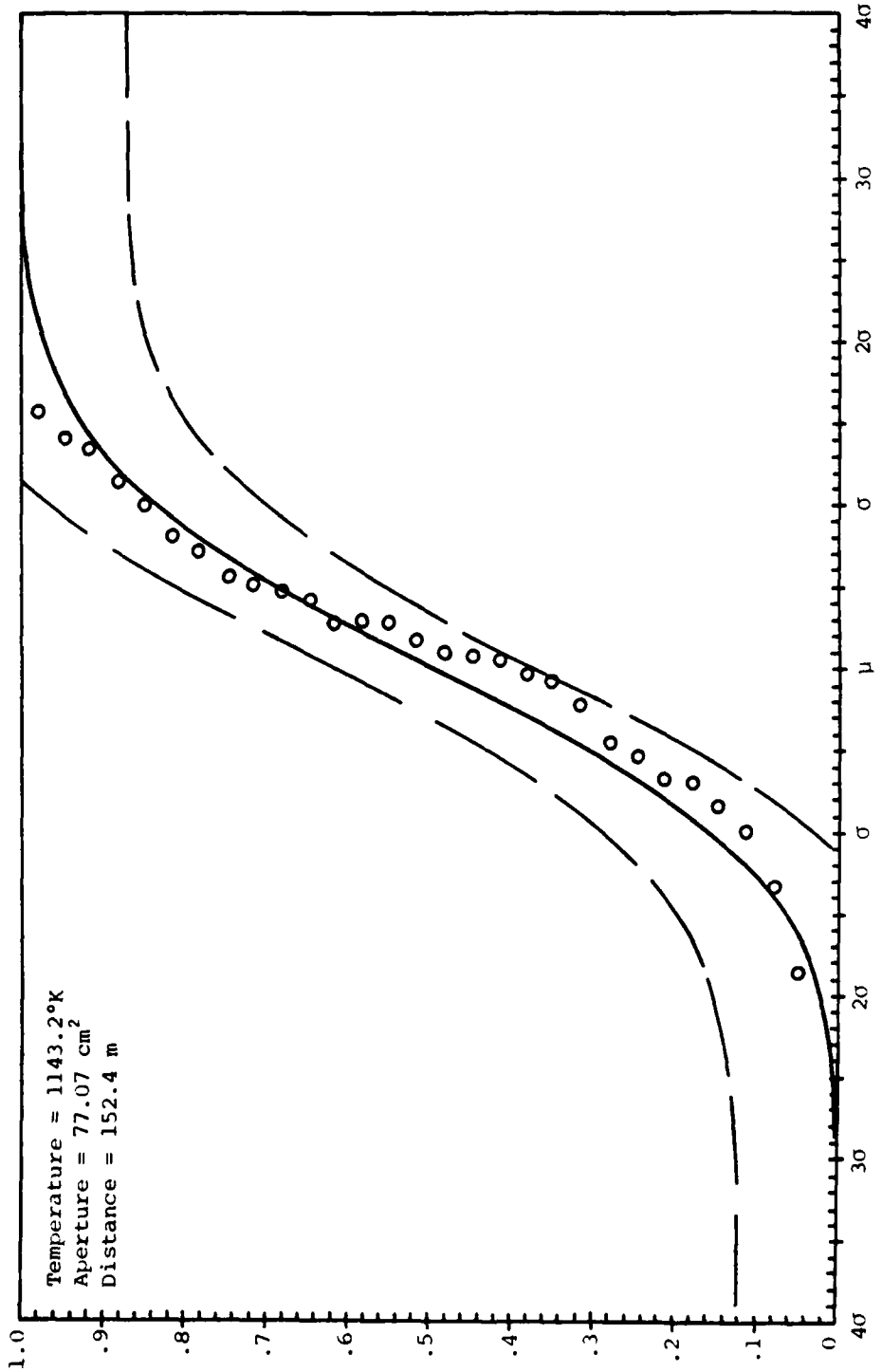

Figure 12. Kolmogorov-Smirnov Test of Normal Ogive Curve for China Lake Data Set With 80% Confidence Level.

A Mathematical Model for Data Variability

The data matrix upon which this study is based consists of 45 data cells. Each cell is determined by three unique values — true temperature, true aperture, and true distance — which correspond to a unique true value of iradiance H_T. Within each cell is a sample of about 30 measured values of irradiance H_M drawn from an infinite population of possible measurement values for the cell. The sample within each data cell has been characterized by the following statistics:

$\bar{H}_M$, the sample mean

S_H, the sample standard deviation

V_H, The sample coefficient of variation*

These values are point estimates of the characteristics of the infinite population of possible measurement values for the cell from which the sample was drawn. The characteristics of the infinite population are:

μ_H, the population mean

σ_H, The population standard deviation

ν_H, the population coefficient of variation*

Values are given for the coefficients of variation for the China Lake data samples in Table 7 and for the White Sands data samples in Table 8. Standard deviation values are listed for convenience. The values listed within the tables for the coefficients of variation are to be used with the factor 10^{-2} as indicated by the column heading. Therefore they may be read directly as percentage variation.

The percentage variation differs from cell to cell and, in general, decreases with increasing mean measured irradiance. A mathematical model relating measurement variability to the measured parameter will now be proposed as an explanation for the behavior of the data.

The noise in an IR measurement system can be described in three basic categories:

1. Noise due to variations in the background against which the measured object is viewed.
2. Noise due to radiation within the system optics.
3. Thermal detector noise.
4. Noise due to random effects associated with the circuitry which transforms the detector response to a system output.

The first type of noise can be reduced by various discrimination techniques, and the second and third by cooling the system. The fourth type is a characteristic of the measurement system and will respond only to system modification.

*Coefficient of variation is one measure of the relative dispersion of a sample or a population. It is defined as the standard deviation divided by the mean.

Table 7. Variability of China Lake Data.

Distance, m	Temperature, °K	Aperture, cm^2	Mean measured irradiance, watts/cm^2 x 10^{-10}	Standard deviation in watts/cm^2 x 10^{-10}	Coefficient of variation, pure x 10^{-2}
152.40					
	804.40	77.070	224.36	7.058	3.15
	804.70	126.700	359.82	8.430	2.34
	986.20	5.067	26.50	3.249	12.26
	985.70	29.200	171.14	6.550	3.83
	986.20	77.070	472.52	9.895	2.09
	1126.20	5.067	53.89	3.584	6.65
	1142.70	29.200	334.98	7.852	2.34
	1143.20	77.070	898.02	23.715	2.64
	1148.20	126.700	1462.2	22.582	1.54
	1126.20	5.067	56.68	4.294	7.58
	1142.70	29.200	356.46	7.209	2.02
	1143.20	77.070	951.69	25.056	2.63
	1148.20	126.700	1549.3	25.314	1.63
60.96	806.20	5.067	94.47	7.187	7.61
	806.20	29.200	528.70	8.783	1.66
	806.20	72.450	1263.5	15.216	1.20
	806.20	101.300	1762.4	19.829	1.12
	993.20	5.067	233.70	6.093	2.61
	988.20	29.200	1303.4	13.581	1.04
	994.20	101.300	4468.5	31.233	.70
60.96	1140.20	5.067	411.06	10.130	2.46
	1145.70	29.200	2283.3	23.335	1.02
	1141.50	101.300	7770.4	99.148	1.28
30.48	805.20	5.067	375.55	14.295	3.81
	805.20	29.200	2157.9	16.684	.77
	805.20	77.070	5837.1	28.900	.50
	805.20	126.700	8338.9	29.352	.35
	994.20	5.067	965.23	12.191	1.26
	993.20	29.200	5387.1	34.914	.65
	990.20	77.070	14352.	39.657	.28
	990.20	126.700	20855.	64.258	.31
	1143.20	5.067	1687.4	12.995	.77
	1143.20	29.200	9105.2	31.395	.34
	1154.70	77.070	25715.	78.698	.31
	1160.70	126.700	37878.	89.139	.24

Table 8. Variability of White Sands Data.

Distance, m	Temperature, °K	Aperture, cm^2	Mean measured irradiance, watts/cm^2 x 10^{-10}	Standard deviation in watts/cm^2 x 10^{-10}	Coefficient of variation, pure x 10^{-2}
155.0	950.26	0.713	4.45	.177	3.99
	950.26	5.067	31.79	.381	1.20
	950.26	20.270	124.34	.909	.73
	950.26	45.600	274.97	.892	.32
	1155.86	0.713	9.18	.172	1.87
	1155.86	5.067	64.28	.720	1.12
	1155.86	20.270	257.12	2.725	1.06
	1155.86	45.600	571.76	3.426	.60
	1423.76	20.270	486.78	3.514	.72
	1423.76	45.600	1148.8	8.100	.70

The postulate is stated that for any individual measurement

$$H_M = H_T + \epsilon_p + \epsilon_N$$

where

H_M is the measured value of irradiance

H_T is the true value of irradiance (an unknown constant)

ϵ_p and ϵ_N are statistically independent, random variables such that

$$\epsilon_p = N[(0, \rho H_T]^*$$ and

$$\epsilon_N = N[f(H_B), \sigma_N]$$

where H_B is the irradiance due to background effects.

The error term ϵ_p is descriptive of the measurement system behavior with respect to the magnitude of the measured parameter, and in fact the standard deviation of the possible infinite population of ϵ_p values is proportional to the measured parameter by a constant coefficient ρ. The error term ϵ_N includes the noise which is inherent in the procedure no matter what the value of the measured parameter is. All system bias is included in the mean value of the infinite population of possible ϵ_N values.

*This is read "ϵ_p is normally distributed with a mean of 0 and a standard deviation ρH_T."

The noise is the result of all contributing physical factors characteristic of the system, and is of the form

$$\epsilon_N = \epsilon_{N1} + \epsilon_{N2} + \epsilon_{N3} + \ldots$$

where the ϵ_{Ni} are all statistically independent, random variables, but this does not alter the generality of the present model development. However, it does indicate the potential for noise reduction by identifying and reducing contributing system effects.

The measurement variance σ_H^2 of an infinite population of possible measurements H_M can be expressed as the sum of the variances of the error terms

$$\sigma_H^2 = \rho^2 H_T^2 + \sigma_N^2$$

since H_T is a constant. Furthermore, if we denote the mean of the noise distribution, which we have included to account for bias due to background effects and system characteristics, by the constant B, then

$$\mu_H = H_T + B, \text{ or } H_T = \mu_H - B$$

Values of sample standard deviation, S_H, and mean measured irradiance, $\bar{H}_M$, have been used as point estimates of σ_H and μ_H in graphing this relationship. The graphs for the China Lake data are shown in Figures 13, 14, and 15. The White Sands data are graphed in Figure 16.

The postulation of this mathematical model for measurement variance in an IR measuring device is not unrealistic. The mathematical expression for error proportional to the measured parameter has been applied to other measurement processes, one such being electrical measurements, in which the noise term is the familiar "Johnson noise", where noise power is proportional to resistance and absolute temperature over a limited range of observations.*

Background Effects and System Noise

The acceptance of the mathematical model postulated in the preceding section as an appropriate description of the measurement variance experienced during the use of these interferometers will depend on future observations. The data matrix used for the present study is too small to yield conclusive results. In particular, a much more detailed data base would be needed at a low value of irradiance to accurately determine the limiting value of S_H as irradiance decreases.

If the postulated model is accepted and sample statistics are used as estimates of the measurement population characteristics, the relationship has the form

$$S_H^2 = \rho^2 (\bar{H}_M - B)^2 + S_N^2$$

*For a discussion of Johnson noise, see Reference Data for Radio Engineers, Howard W. Sams & Co., 1975, Article 17-12.

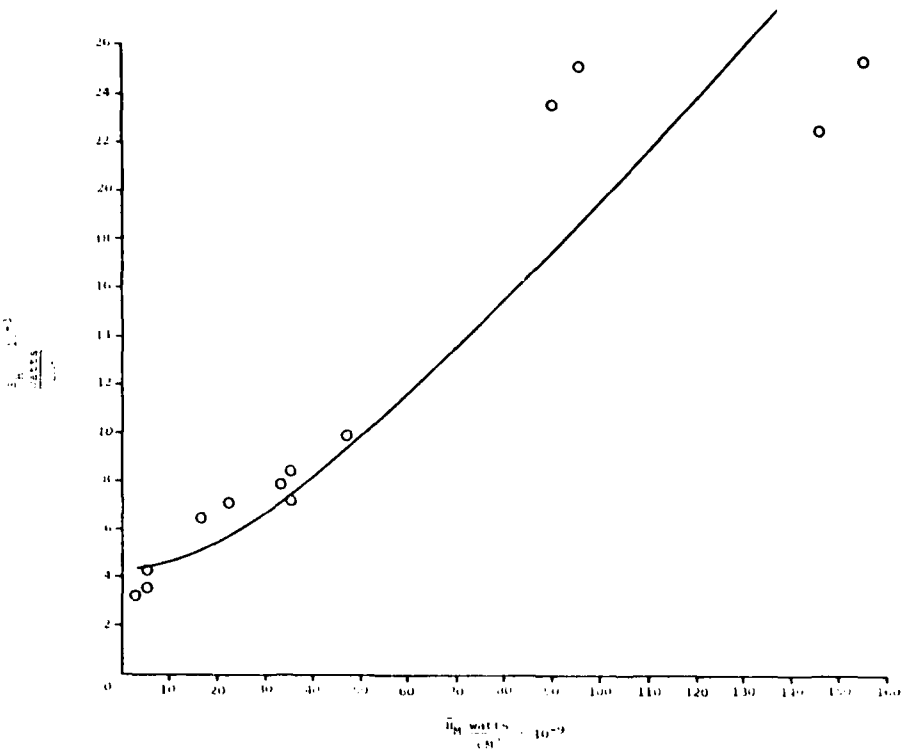

Figure 13. Sample Standard Deviation as a Function of Mean Measured Irradiance, China Lake Data Measured at 152.4 Meters.

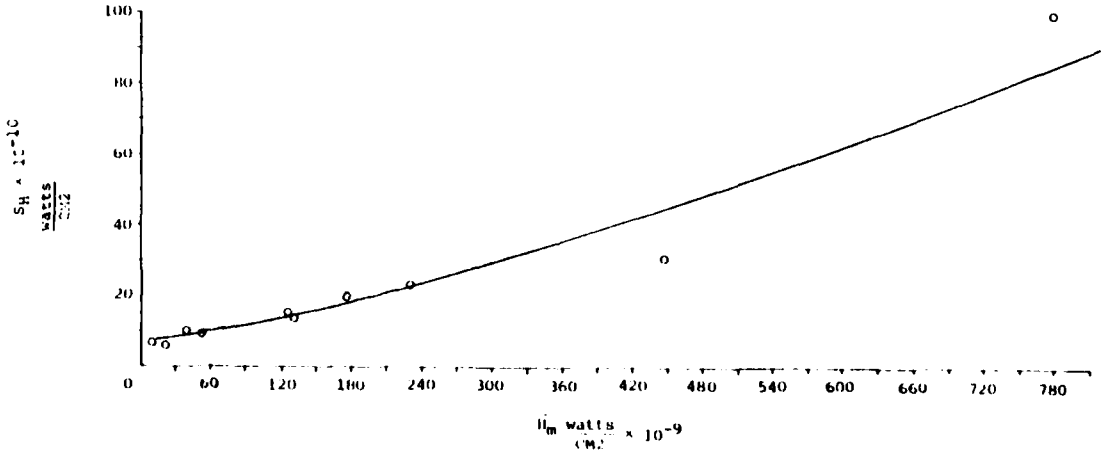

Figure 14. Sample Standard Deviation as a Function of Mean Measured Irradiance, China Lake Data Measured at 60.96 Meters.

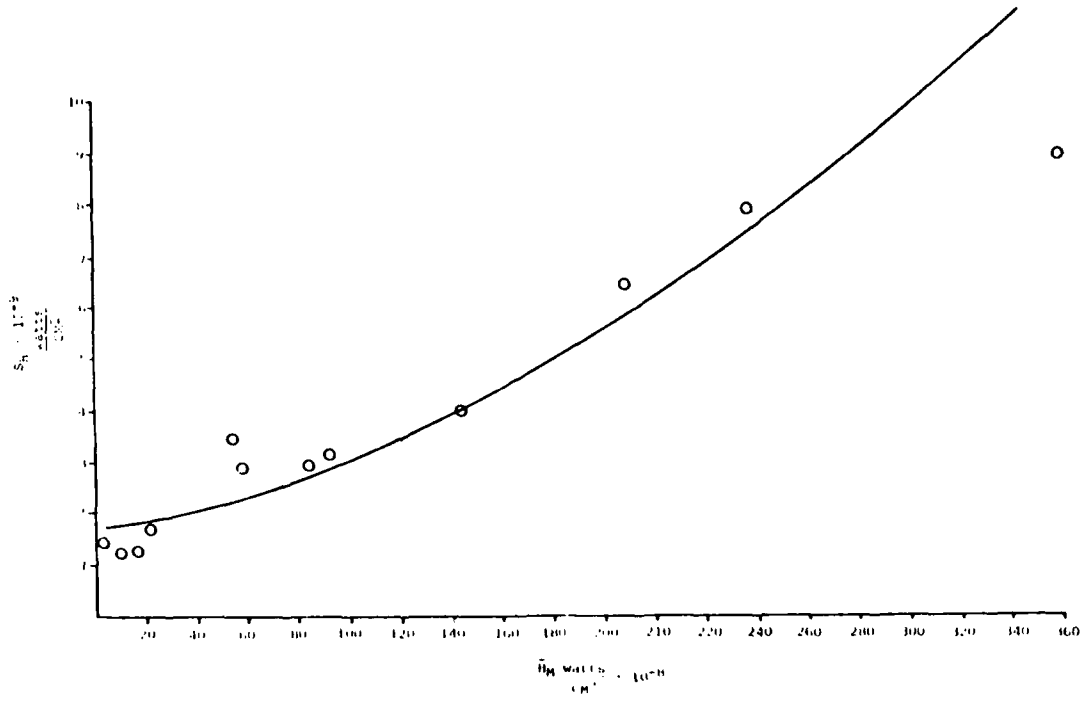

Figure 15. Sample Standard Deviation as a Function of Mean Measured Irradiance, China Lake Data Measured at 30.48 Meters.

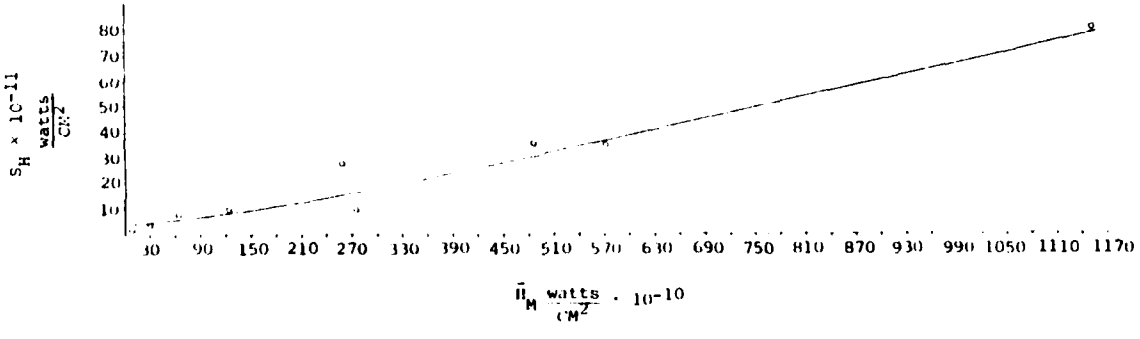

Figure 16. Sample Standard Deviation as a Function of Mean Measured Irradiance, White Sands Data Measured at 155 Meters.

When this is rewritten as

$$\frac{S_H^2}{S_N^2} - \frac{(\bar{H}_M - B)^2}{(S_N/\rho)^2} = 1$$

it has the form of a hyperbola with branches above and below the $\bar{H}_M$ axis whose center is the point (B,O). In actual practice

$$\bar{H}_M \geq B, \text{ and } S_H \geq 0$$

so that only the right half of the upper branch of the hyperbola could ever be generated by measurement data as shown in Figure 17.

The value of S_N is the minimum value of S_H which can be obtained as $\bar{H}_M$ is decreased. The limiting value of the slope of the curve as $\bar{H}_M$ is increased (which is the slope of the asymptote) is ρ. The value of B may be estimated from the intersection of the hyperbolic asymptote with the axis of abscissas. These mathematical concepts could be used by measurement facilities to estimate the standard deviation of the noise error, the background term, and the fractional coefficient in the percentage error term for their measurement equipments.

Coefficient of Variation

The equation developed to relate measurement variance to mean measured irradiance

$$S_H^2 = \rho^2(\bar{H}_M - B)^2 + S_N^2$$

may be written

$$\frac{S_H^2}{\bar{H}_M^2} = \rho^2 \left[\frac{\bar{H}_M^2 - 2\bar{H}_M B + B^2}{\bar{H}_M^2} \right] + \frac{S_N^2}{\bar{H}_M^2}$$

which in terms of the coefficient of variation V_H gives

$$V_H = \left[\rho^2 \left(1 - \frac{2B}{\bar{H}_M} + \frac{B^2}{\bar{H}_M^2} \right) + \frac{S_N^2}{\bar{H}_M^2} \right]^{1/2}$$

As $\bar{H}_M$ decreases to B, the first term approaches 0, and the value of V_H tends toward the coefficient of variation due to noise.

For $\bar{H}_M >> B$ (and consequently $\bar{H}_M >> S_N$), the value of V_H approaches ρ, which is the postulated fractional error in measurement of the true irradiance. Plots of coefficient of variation as a function of mean measured irradiance are therefore a means for determining the value of ρ by inspection. These plots are given in Figures 18, 19, and 20 for the China Lake data and in Figure 21 for the White Sands data.

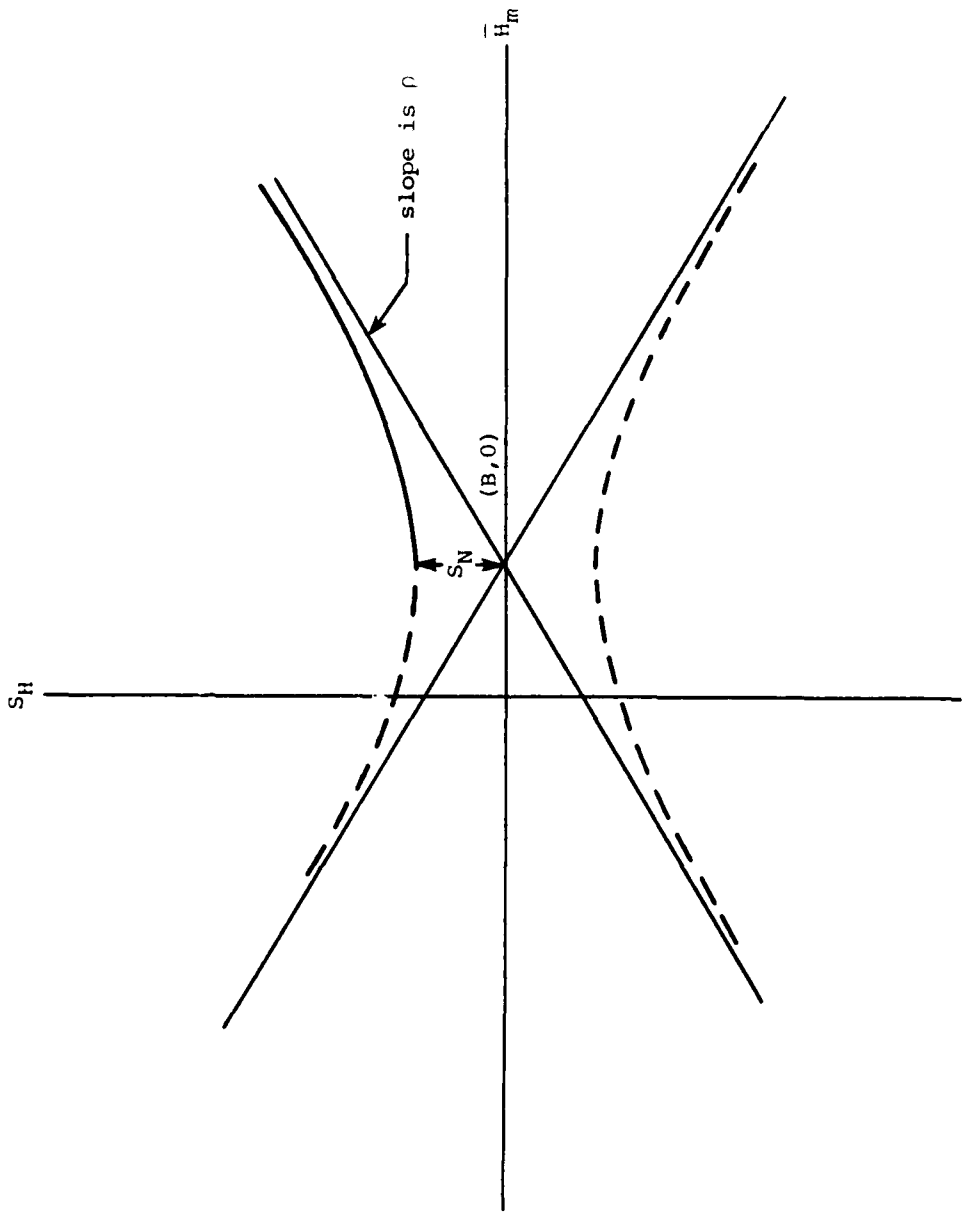

Figure 17. Experimental Values Represent an Hyperbolic Segment.

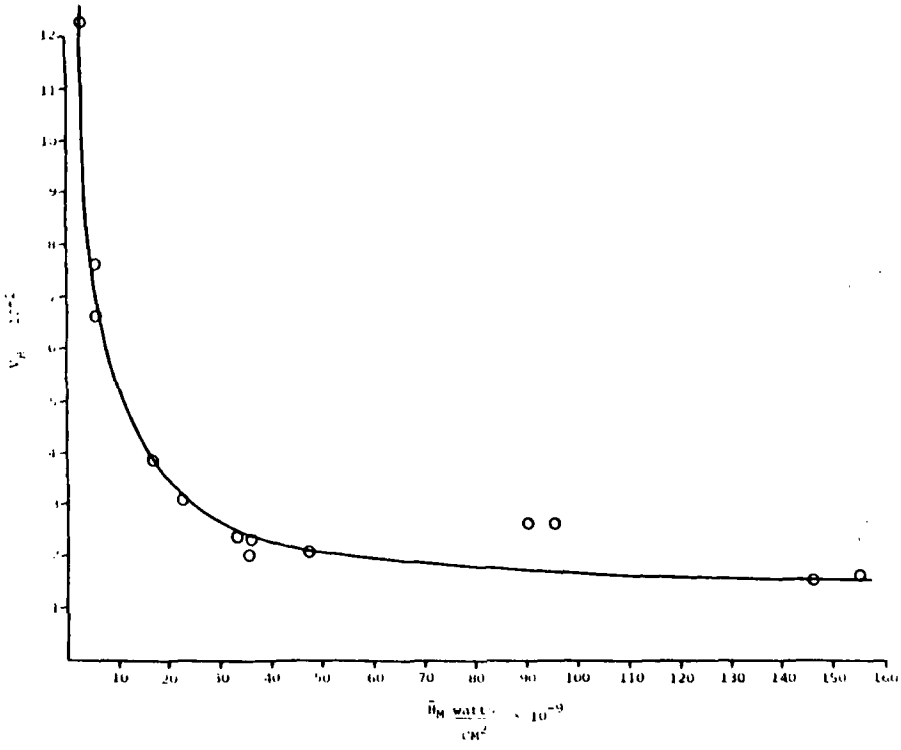

Figure 18. Sample Coefficient of Variation as a Function of Mean Measured Irradiance, China Lake Data Measured at 152.4 Meters.

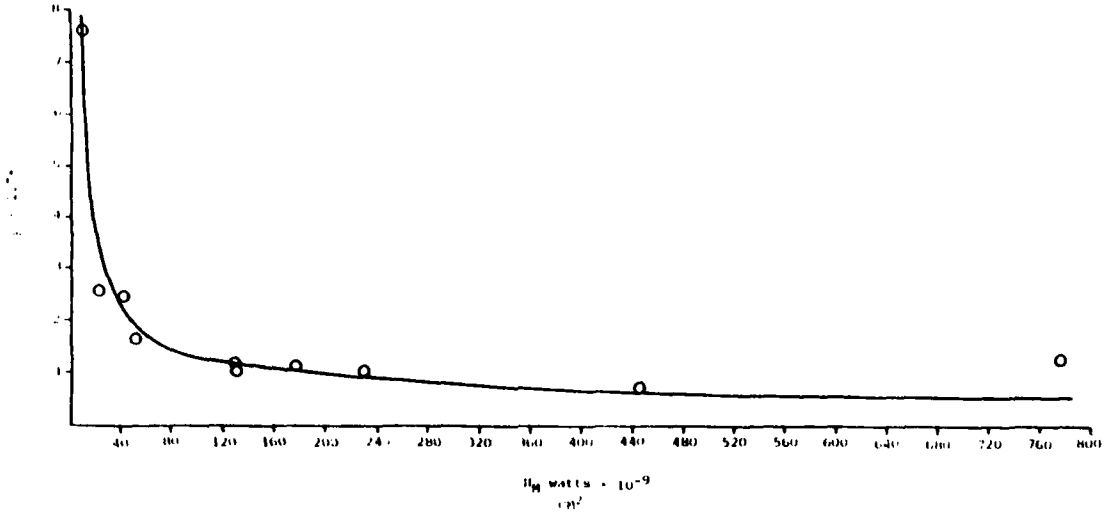

Figure 19. Sample Coefficient of Variation as a Function of Mean Measured Irradiance, China Lake Data Measured at 60.96 Meters.

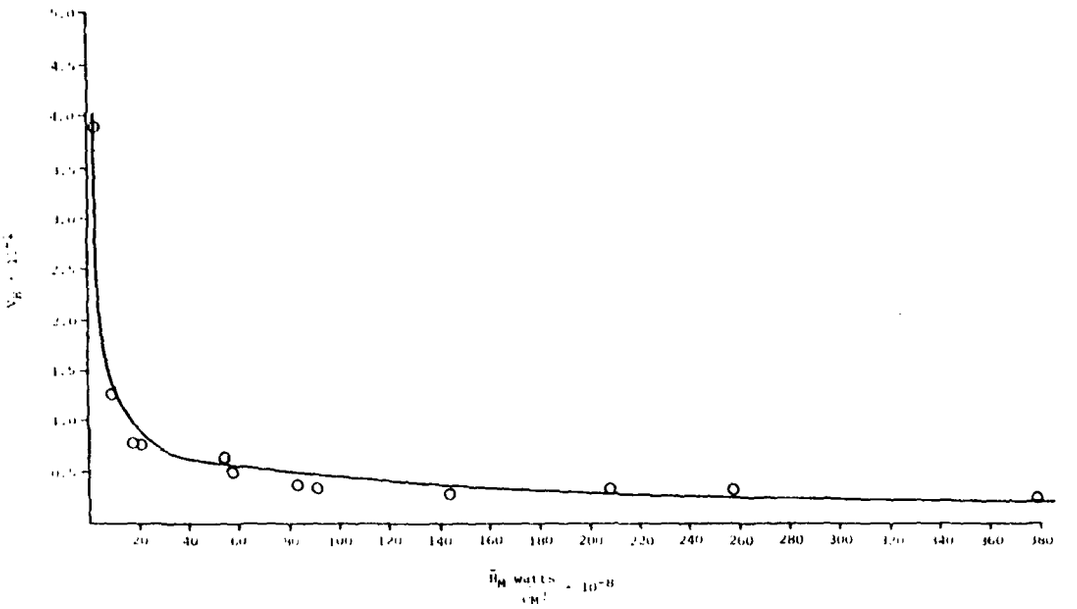

Figure 20. Sample Coefficient of Variation as a Function of Mean Measured Irradiance, China Lake Data Measured at 30.48 Meters.

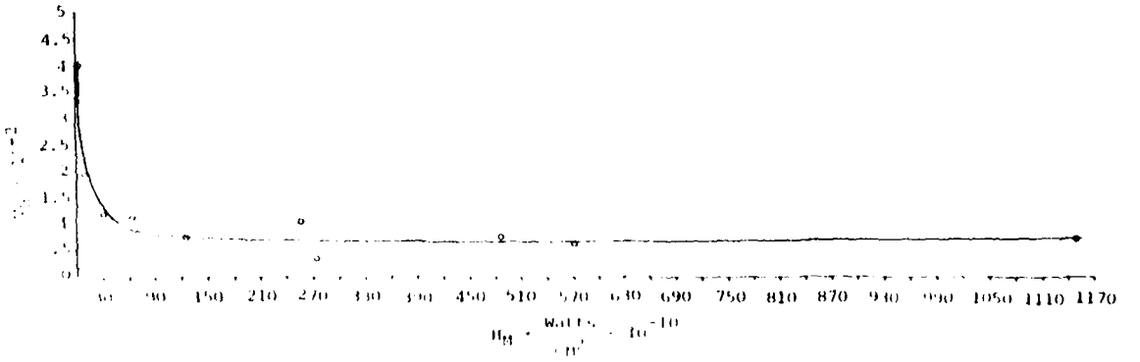

Figure 21. Sample Coefficient of Variation as a Function of Mean Measured Irradiance, White Sands Data Measured at 155 Meters.

Computing Percentage Variability and System Noise

If the mathematical statement

$$S_H^2 = \rho^2(\bar{H}_M - B)^2 + S_N^2$$

is a reasonable description of the measurement variability, and if we can assume that both background and system bias are very small, we may write

$$S_H^2 \simeq \rho^2 \bar{H}_M^2 + S_N^2$$

A graph of S_H^2 as a function of $\bar{H}_M^2$ would then be a straight line with slope ρ^2 and intercept S_N^2. This straight line can be determined analytically by using the method of least squares to fit the data.

A linear correlation coefficient can be computed for the variables

$$Y = S_H^2 \text{ and } X = \bar{H}_M^2$$

to determine the appropriateness of the assumption that

$$Y = f(X)$$

is a straight line. This correlation coefficient is defined as

$$r = \frac{\Sigma(X - \bar{X}) \cdot (Y - \bar{Y})}{\{[\Sigma(X - \bar{X})^2][\Sigma(Y - \bar{Y})^2]\}^{1/2}}$$

and has values close to +1 or -1 if a pronounced linear relationship does exist.* Values close to zero indicate almost no linear correlation between the variables.

This analysis was performed on the 35 data cells from China Lake and the 10 data cells from White Sands. The White Sands data yielded striking results immediately, with a correlation coefficient of .99. First efforts with the China Lake data showed almost no linear correlation when all the data cells were evaluated together. However, when the China Lake data cells were evaluated separately by distance, they showed strong linear correlation.

The strongest linear correlation shown by the China Lake data was .97 at a distance of 60.96 meters. The correlation for 30.48 meters was about .96; for 152.4 meters the coefficient was about .86.

The results of this linear correlation analysis are listed in Table 9. There is a strong inference that ρ is a function of distance, which increases as distance increases. This suggests that for small values of H_T, σ_H^2 may decrease as $\rho^2 H_T^2$ but take some minimum "noise" value. The scope of the present measurement program does not allow final resolution of this question.

*Here $\bar{X}$ is the mean of the abscissas and $\bar{Y}$ is the mean of the ordinates for the data points fitted.

Table 9. Fractional Variability From Linear Correlation of S_H^2 and $\bar{H}_M^2$.

Distance, m	Number of data points	Correlation coefficient	Slope	Fractional variability
China Lake				
30.48	12	0.95903	0.05853×10^{-4}	0.2419×10^{-2}
60.96	10	0.97276	1.55616×10^{-4}	1.2474×10^{-2}
152.4	13	0.85806	2.71528×10^{-4}	1.6478×10^{-2}
White Sands				
152.4	10	0.99373	0.49159×10^{-4}	0.7011×10^{-2}

Effects of Noise on Measurement System Output

The effect of noise relative to the signal strength at the detector of the measurement system is clearly seen in Figures 22, 23, and 24. These figures show graphs of apparent spectral radiant intensity for strong, moderate, and weak signals selected from the White Sands data set.

COMPARISON OF MEASURED AND CALCULATED VALUES

Significant Systematic Differences

The analysis described in this section was performed to determine whether a significant systematic difference exists between the true but unknown mean of the possible measurement population and the irradiance value calculated from measured values of temperature ($T + \Delta T$), aperture ($A + \Delta A$), and distance ($D + \Delta D$). The sample means $\bar{H}_M$ were used as point estimates of the measurement population means μ_{H_i} for the data cells in investigating significant difference. The emissivity of the blackbody source cannot be greater than unity, but may be noticeably less than unity. Emissivity is taken to be unity in calculating a value of irradiance, so that a measured value of irradiance resulting from an emissivity less than unity would be smaller. Also, a fractional atmospheric transmission factor affects the measured value of irradiance, but is not accounted for in the calculated value. This would also tend to make the measured value less than the calculated value.

DATA> P78804.DBE SCAN>11 KIND>1 MB NOF2 >3044 ITYPE>2
BG > P78801.DB SCAN>11 KIND>2 COBLE>0 NOF1 >2102 NOM >7418
LN? > SCAN>0 KIND>1 POTRO>1.00
CAL > P78000.CB SCAN>4 KIND>3

MEASUREMENT CONDITIONS
DATE:17 10 78
TIME:1 :14:8 .79

INTEGRATION
BANDX>(3.00 -4.00) +0.276132 02

TARGET CONDITIONS
AZ: -158.
EL: -2.
AZ ASPECT ANGLE: 16.09
EL ASPECT ANGLE: -6.30
RANGE: 155.00

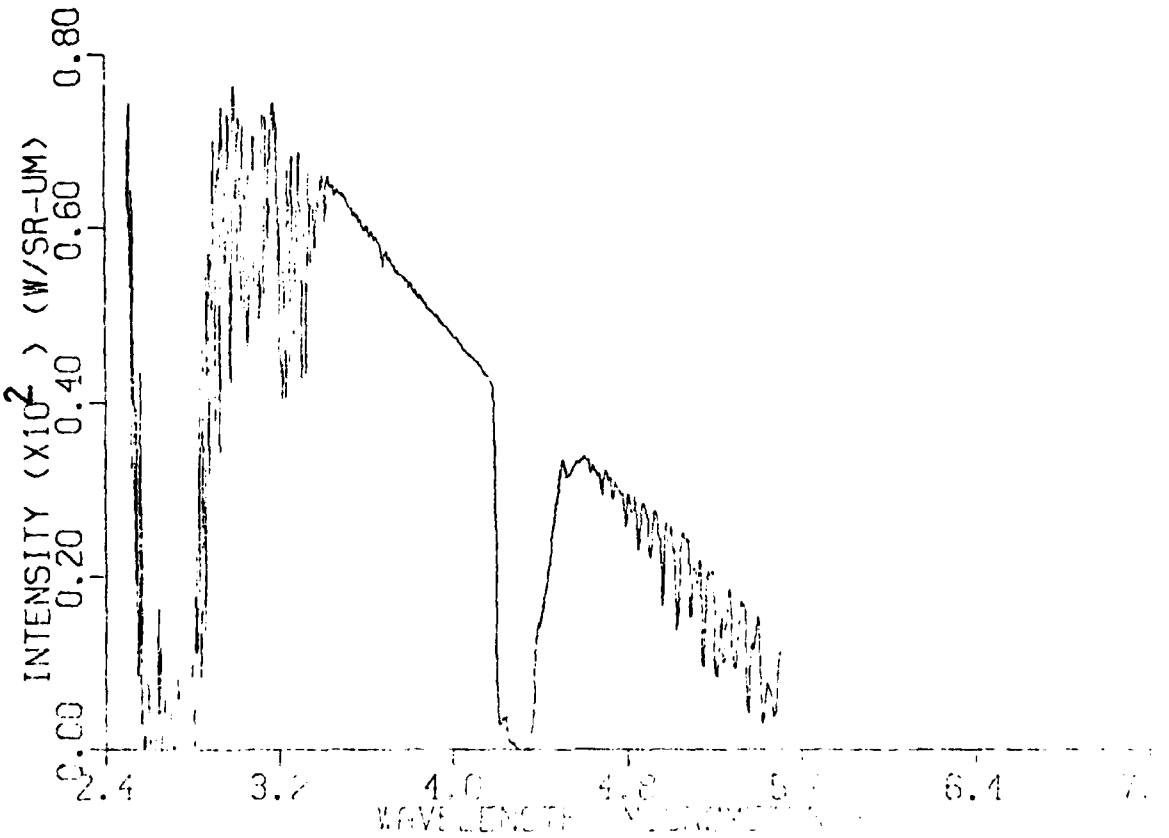

Figure 22. Apparent Spectral Radiant Intensity, Calculated Value of Irradiance is 1.11 E-07.

DATA> P78A15.DBS SCAN>11 KIND>1 MB NAF2 >3048 ITYPE>2
BG > P78A15.DB SCAN>11 KIND>2 CORDD>0 NFFT >8192 NUM >7413
LN2 > SCAN>0 KIND>1 PCTBG>1.00
CAL > P78A31.DB SCAN>5 KIND>3

MEASUREMENT CONDITIONS
DATE:17 [illegible]
TIME:0 [illegible]

INTEGRATION
BAND> 3.50 -4.00 [illegible]

TARGET CONDITIONS
AZ: -108.
EL: -2.
AZ ASPECT ANGLE: 66.34
EL ASPECT ANGLE: -0.00
RANGE: 155.00

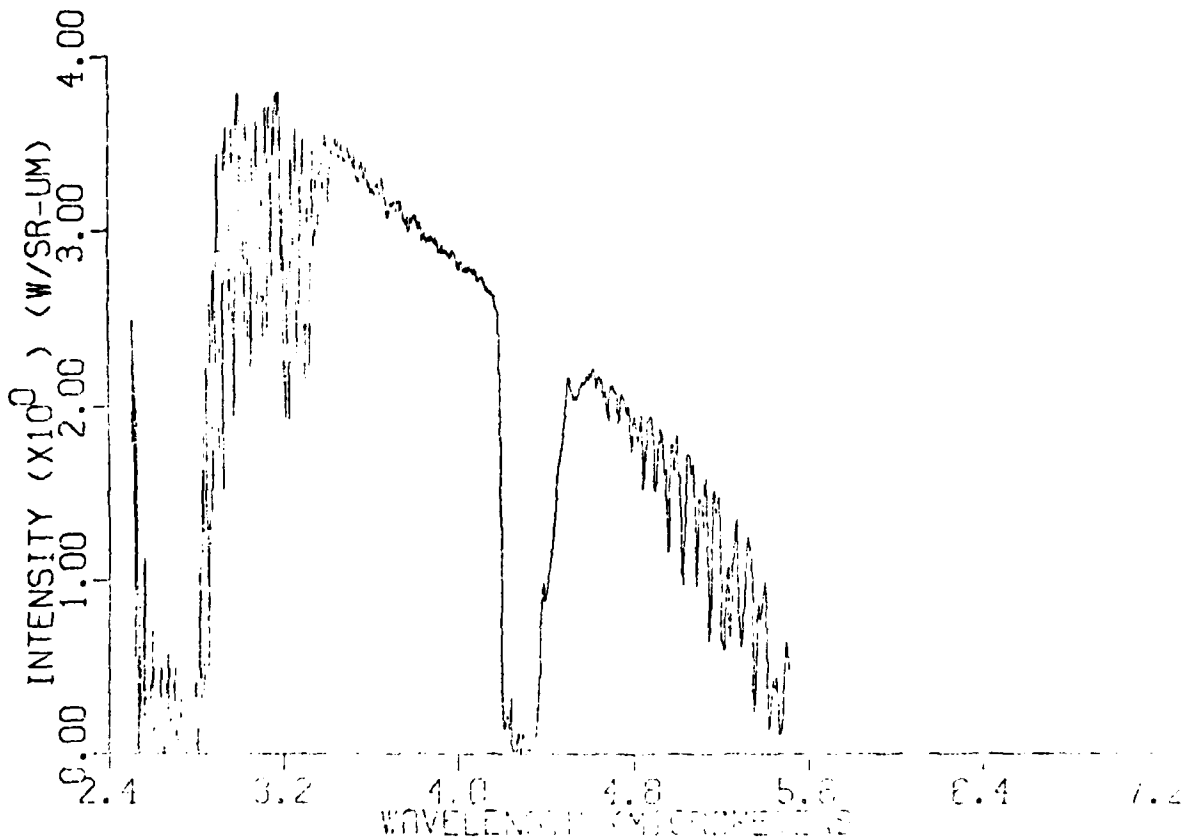

Figure 23. Apparent Spectral Radiant Intensity, Calculated Value of Irradiance is 6.36 E-09.

DATA> P78A05.DBE	SCAN>13	KIND>1	M6	NAP2 >3344	ITYPE>2
BG > P78A05.DB	SCAN>13	KIND>2	CØADD>0	NFFT >8192	NUM >7488
LN2 >	SCAN>0	KIND>1	PCTBG>1.00		
CAL > P78A01.CB	SCAN>5	KIND>3			

MEASUREMENT CØNDITIØNS
DATE:17 10 78
TIME:1 :50:52.79

INTEGRATIØN
BANDXX(3.50 -4.00) +0.103975 00

TARGET CØNDITIØNS
AZ: -108.
EL: -1.
AZ ASPECT ANGLE: 66.30
EL ASPECT ANGLE: 0.02
RANGE: 155.00

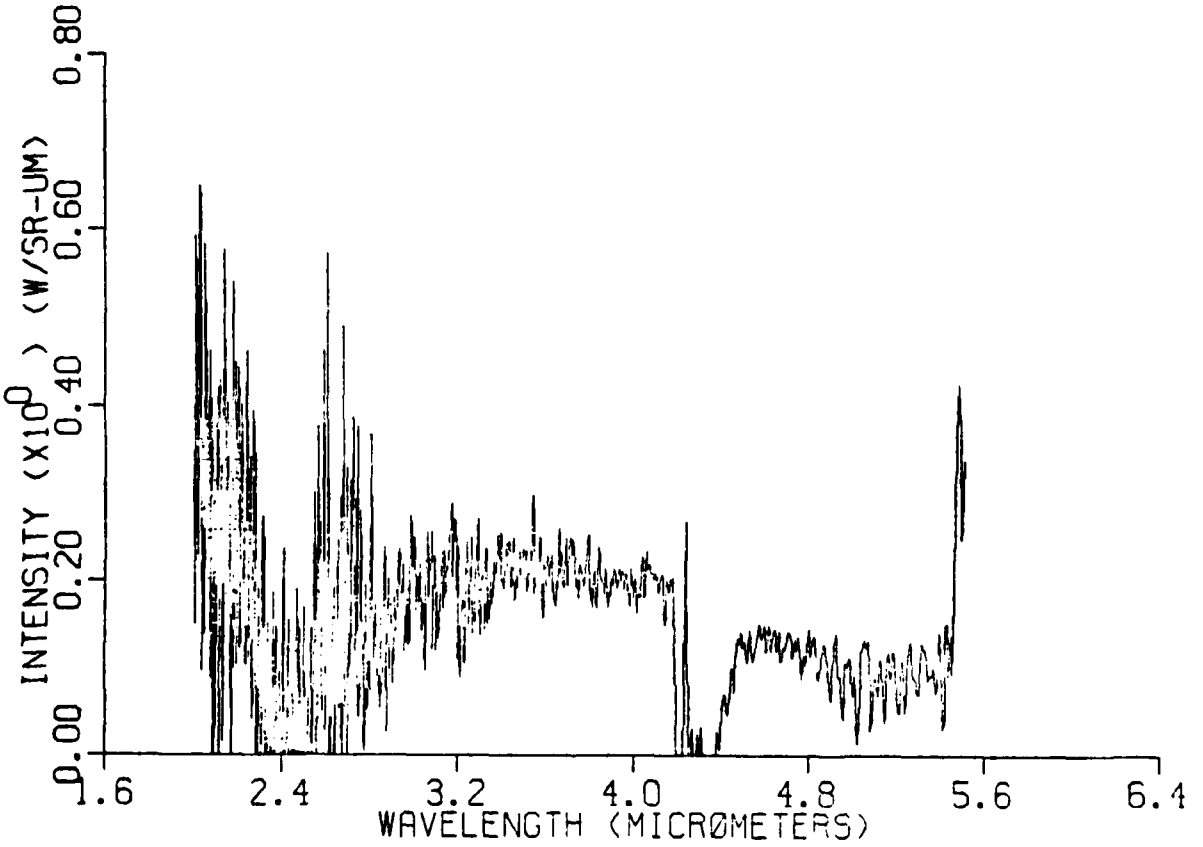

Figure 24. Apparent Spectral Radiant Intensity, Calculated Value of Irradiance is 4.27 E-10.

For these reasons, the values of $\bar{H}_M - H_C$ were expected to be negative and to indicate a definite bias showing calculated irradiance to be systematically greater than mean measured irradiance. In fact, many of the values were found to indicate with 99% confidence that a definite positive bias exists. This result must derive from one or more of the following effects:

1. Error in the temperature measurement, ΔT
2. Error in the aperture measurement, ΔA
3. Error in the distance measurement, ΔD
4. Error in the calibrated system response, ΔR.

Since the potential for all these effects is present, it cannot be said conclusively which effects are involved. However, some inferences may be drawn from examination of the data. The method will now be explained.

The experimental data from NWC and OMEW were examined to determine whether a significant *systematic* difference between measured and calculated irradiance values truly exists. This determination was made by calculating the t-statistic for each data cell and comparing its value to percentile points of the Student t-distribution.

The assumption is made that the random variation $[H_M - H_C]_{random}$ is normally distributed. Within each data cell there are N (usually 30) measured values of H_M and one calculated value H_C. The true, but unknown, mean of the infinite population of possible measurements H_M is μ_{H_M}. One can never know μ_{H_M}, but it is known that

$$\mu_{H_M} - H_C = f[\Delta T, \Delta A, \Delta D, \tau(D,\lambda), \epsilon, \Delta R(\lambda)]$$

An estimate of μ_{H_M} is made by taking the mean $\bar{H}_M$ of the sample of N measurements then symmetric confidence limits on the estimate $\bar{H}_M$ can be determined.

The next step is to decide whether the difference $[\bar{H}_M - H_C]$ significantly exceeds the data spread introduced by the random component of error. That is, does a significant component $[\bar{H}_M - H_C]_{systematic}$ exist above and beyond the variability $[H_M - H_C]_{random}$ which one expects measurement system fluctuations to cause? Next comes the crucial step in the thought process. If no systematic difference exists, and the difference $[H_M - H_C]$ is completely random, then $\mu_{H_M} = H_C$ cannot be rejected as the true but unknown mean of the infinite population of all possible measurements of H_M. More formally, a statistical hypothesis is formulated that can be tested by established techniques.

The null hypothesis and its alternative are stated in the format of Neyman-Pearson:

Null hypothesis H_0: $H_C = \mu_{H_M}$

Alternative hypothesis H_1: $H_C \neq \mu_{H_M}$

A statistic is defined for which the distribution is known if H_0 is true. This statistic is

$$t = \frac{\bar{H}_M - H_C}{S_{H_M}} \sqrt{N - 1}$$

where S_{H_M} is the sample standard deviation. (The mean square deviation formula for S_H^2 was used in this computation. Using the unbiased estimator $(\frac{N}{N-1})S_H^2$ does not change the results.) The value of t was computed for each data cell and compared to the density function for t's corresponding to samples of size N drawn from the normal distribution. The null hypothesis was rejected for all cases where the t-value was shown to be greater than the values for 99% of the t-population.

Values of the t-statistic for the China Lake and White Sands data are given in Tables 10 and 11 respectively. For data samples having thirty members, the null hypothesis was rejected for t-values exceeding 2.76.

Inspection of Systematic Difference

In general, any significant systematic difference between measured and calculated irradiance values will be the result of some combination of factors such as

ϵ, the blackbody emissivity

τ, the atmospheric transmission

which will tend to make $\bar{H}_M$ less than H_C, and the errors in the measurements of temperature, aperture, distance, and system response, which have the potential for affecting the value $[\bar{H}_M - H_C]$ in either a positive or a negative sense. Usually it will not be possible to determine which factors prevail in a particular instance.

Inspection of the data in Table 12, which contains $[\bar{H}_M - H_C]$ values for the 30.48 meter distance data from China Lake, suggests that inspection of systematic bias patterns may be helpful in some cases. Although all $[\bar{H}_M - H_C]$ values might be expected to be negative due to transmission and emissivity effects, the data show a distinct correlation of bias to aperture. The probability (P) of this suggestive pattern of signs (positive and negative bias) resulting from fortuitous circumstance is:

$$P = \frac{1}{2^{12}}$$

Therefore one might reasonably postulate that the first aperture was cut too large, the second too small, the third too large, and the fourth too small, and that these results prevailed throughout the measurement process.

Table 10. Values of the t Statistic for the China Lake Data.

Distance, m	Nominal temperature, °K	Aperture, cm^2					
		5.067	29.200	77.070	77.450	101.300	126.700
30.48	805	0.124	-1.445	24.631			-194.72
60.96	805	0.079	-9.426	•	-30.872	-34.296	•
152.40	805			-2.200			-9.328
30.48	990	10.320	-3.353	34.110			-198.85
60.96	990	-0.832	-8.831			-42.225	•
152.40	990	-16.858	-32.431	-45.763			
30.48	1150	43.972	-3.057	54.592			-236.34
60.96	1150	10.228	-3.469			-5.652	•
152.40	1150	-9.449	-20.487	-15.038			-35.273
152.40	1150	-4.336	-5.995	-2.501	-	-	-12.620

•Data taken at aperture in adjacent column.

Table 11. Values of the t Statistic for the White Sands Data at a Distance of 155 Meters.

Nominal temperature, °K	Measured aperture values (A + ΔA), cm^2			
	0.713	5.067	20.270	45.600
950.26	5.498	20.602	17.416•	10.745
1155.86	7.645	5.133	5.399	-.985•
1423.76			-8.668	27.870

•Data set has only 29 members.

Inspection of systematic bias could be routinely practiced by measurement facilities as a check on measured values of temperature, aperture, and distance. Changes in bias with system recalibration might serve as a check on the response error. Patterns such as the one shown in Table 12 are not conclusive, but will provide insights for further investigations.

Note that this inspection technique is in reality just a version of the graphical method explained under *Inspection of Measurement Data by Graphing* where for positive values of $|H_M - H_C|$ the data points would lie above the line $H_M = H_C$.

Table 12. Values of $|\bar{H}_M - H_C|$ for the China Lake Data at a Distance of 30.48 Meters.

Nominal temperature, °K	Measured aperture values (A + ΔA), cm^2							
	5.067		29.200		77.070		126.700	
805	3.3	E-11	-4.4	E-10	1.30	E-08	-1.04	E-07
990	2.30	E-09	-2.14	E-09	2.47	E-08	-2.33	E-07
1150	1.04	E-08	-1.75	E-09	7.85	E-08	-3.85	E-07

ANALYSIS OF EXPERIMENTAL THEORY

REPRODUCIBILITY OF THE EXPERIMENT

The Blackbody Experiment

In the two preceding chapters, the problems of sample-to-sample variability and bias were examined with respect to data describing blackbody emissions. In this section the uncertainty in reproducing the physical conditions or defining parameters, which uniquely define the experiment, is expressed. This is an application of the concepts developed in the section entitled *Quantifying Reproducibility*.

The reader should be aware that the mathematical derivations in this chapter involve many assumptions whose verifications are beyond the scope of this effort. The analysis is presented to show how the uncertainty associated with reproducing an experiment can be determined from the defining equation for the experiment, but does not pretend to account for all possible contributing effects. In any event, the merit of this discussion is the demonstration of the methodology, since the actual application would be completely different for any operating aircraft, which is the problem of interest in the overall study of which this report forms a part.

The Defining Equation

The defining equation for reproducibility of the blackbody experiment has been given for the true value of irradiance at the collecting optics of the measurement system as

$$H_T = \frac{A\epsilon}{\pi D^2} \int_{3.5\,\mu m}^{4.0\,\mu m} W(\lambda,T) \cdot \tau(\lambda,D)\, d\lambda$$

Acceptance of this equation implies that all problems with equipment alignment are inherent in apparent aperture and that any variation in beam strength across the collimated beam (for China Lake data) is inherent in apparent emissivity.

Calculated Value of Irradiance

The calculated values of irradiance for this experiment were derived from values of unity for emissivity and atmospheric transmission. The error terms for these parameters are therefore defined as

$$\Delta\epsilon = 1 - \epsilon$$

$$\Delta\tau = 1 - \tau$$

for convenience in computation. The calculated value of irradiance becomes

$$H_C = \frac{(A + \Delta A)(\epsilon + \Delta\epsilon)}{\pi(D + \Delta D)^2} \int_{3.5\,\mu m}^{4.0\,\mu m} W(\lambda, T + \Delta T) \cdot [\tau(\lambda, D + \Delta D) + \Delta\tau(\lambda, D + \Delta D)]\, d\lambda$$

Two algebraic expressions must be developed for use in obtaining a formula for calculated irradiance.

Expression 1:

$$W(\lambda, T + \Delta T) - W(\lambda, T) = \frac{\partial W}{\partial T} \cdot \Delta T$$

$$W(\lambda, T + \Delta T) = \frac{\partial W}{\partial T} \cdot \Delta T + W(\lambda, T)$$

$$\int_{3.5\,\mu m}^{4.0\,\mu m} W(\lambda, T + \Delta T)\, d\lambda = \Delta T \int_{3.5\,\mu m}^{4.0\,\mu m} \frac{\partial W}{\partial T}\, d\lambda + \int_{3.5\,\mu m}^{4.0\,\mu m} W(\lambda, T)\, d\lambda$$

Expression 2:

$$\frac{A + \Delta A}{\pi(D + \Delta D)^2} = \frac{A + \Delta A}{\pi} \left[\frac{1}{D^2 \left(1 + \frac{2\Delta D}{D} + \frac{\overline{\Delta D}^2}{D^2}\right)} \right]$$

$$= \frac{A + \Delta A}{\pi D^2} \left[1 - \frac{2\Delta D}{D} + \frac{3\overline{\Delta D}^2}{D^2} - \frac{4\overline{\Delta D}^3}{D^3} + \text{higher order terms in D and } \Delta D \right]$$

$$= \frac{A}{\pi D^2} - \frac{2A\Delta D}{\pi D^3} + \frac{\Delta A}{\pi D^2} + \text{terms of second order or more}$$

If terms of second order or greater can legitimately be discarded (an assumption that will not be proved or discussed within the scope of this effort) this becomes

$$\frac{A}{\pi D^2}\left(1 - \frac{2\Delta D}{D} + \frac{\Delta A}{A}\right)$$

Now the equation for calculated irradiance can be written

$$H_C = \frac{A + \Delta A}{\pi(D + \Delta D)^2} \int_{3.5\,\mu m}^{4.0\,\mu m} W(\lambda, T + \Delta T)d\lambda$$

since

$$\epsilon + \Delta\epsilon = 2$$

$$\tau + \Delta\tau = 1$$

Using the two expressions just developed, this can be rewritten

$$H_C = \frac{A}{\pi D^2}\left[1 - \frac{2\Delta D}{D} + \frac{\Delta A}{A}\right]\left[\Delta T \int_{3.5\,\mu m}^{4.0\,\mu m} \frac{\partial W}{\partial T} d\lambda + \int_{3.5\,\mu m}^{4.0\,\mu m} W(\lambda, T)d\lambda\right]$$

Continuing to discard terms of second order or greater, this becomes

$$H_C = \frac{A}{\pi D^2}\left[\Delta T \int_{3.5\,\mu m}^{4.0\,\mu m} \frac{\partial W}{\partial T} d\lambda + \int_{3.5\,\mu m}^{4.0\,\mu m} W(\lambda, T)d\lambda\right.$$

$$\left. - \frac{2\Delta D}{D} \int_{3.5\,\mu m}^{4.0\,\mu m} W(\lambda, T)d\lambda + \frac{\Delta A}{A} \int_{3.5\,\mu m}^{4.0\,\mu m} W(\lambda, T)d\lambda\right] .$$

True Value of Irradiance

The equation for true irradiance can be rewritten

$$H_T = \frac{A}{\pi D^2}(1 - \Delta\epsilon) \int_{3.5\,\mu m}^{4.0\,\mu m} W(\lambda, T) \cdot (1 - \Delta\tau)d\lambda$$

which becomes, if second order or greater terms are discarded,

$$H_T = \frac{A}{\pi D^2}\left[\int_{3.5\,\mu m}^{4.0\,\mu m} W(\lambda,T)d\lambda - \int_{3.5\,\mu m}^{4.0\,\mu m} W(\lambda,T)\cdot\Delta\tau d\lambda - \Delta\epsilon \int_{3.5\,\mu m}^{4.0\,\mu m} W(\lambda,T)d\lambda\right]$$

Difference Between Calculated and True Irradiance

The mathematical expression for the difference between calculated and true irradiance ($H_C - H_T$), based only on the assumption that terms of the second order or greater may be discarded, is

$$\frac{A}{\pi D^2}\left[\Delta T \int_{3.5\,\mu m}^{4.0\,\mu m} \frac{\partial W}{\partial T} d\lambda + \frac{\Delta A}{A} \int_{3.5\,\mu m}^{4.0\,\mu m} W(\lambda,T)d\lambda - \frac{2\Delta D}{D} \int_{3.5\,\mu m}^{4.0\,\mu m} W(\lambda,T)d\lambda + \Delta\epsilon \int_{3.5\,\mu m}^{4.0\,\mu m} W(\lambda,T)d\lambda + \int_{3.5\,\mu m}^{4.0\,\mu m} W(\lambda,T)\Delta\tau d\lambda\right]$$

where

$$W(\lambda,T) = \frac{c_1}{\lambda^5} \frac{1}{e^{c_2/\lambda T} - 1}$$

and

$$\frac{\partial W}{\partial T} = \frac{c_1}{\lambda^5} \frac{c_2}{\lambda T^2} \frac{e^{c_2/\lambda T}}{|e^{c_2/\lambda T} - 1|^2}$$

If the errors ΔT, ΔA, ΔD, $\Delta\epsilon$, and $\Delta\tau$ which can occur in the measurement of the defining parameters are all statistically independent, random variables, then the variance of the variable $\Delta H = (H_C - H_T)$ can be expressed as

$$\sigma^2_{\Delta H} = \sigma^2_{\Delta T}(k_T)^2 + \sigma^2_{\Delta A}(k_A)^2 + \sigma^2_{\Delta D}(k_D)^2 + \sigma^2_{\Delta\epsilon}(k_\epsilon)^2 + \sigma^2_{\Delta\tau}(k_\tau)^2$$

where k_T, k_A, k_D, k_ϵ, and k_τ are the algebraic coefficients of the errors ΔT, ΔA, ΔD, $\Delta\epsilon$, and $\Delta\tau$, respectively, in the equation for $(H_C - H_T)$.

Specifically

$$k_T\Delta T = \left[\frac{A}{\pi D^2}\int_{3.5\,\mu m}^{4.0\,\mu m}\frac{c_1 c_2}{\lambda^6 T^2}\,\frac{e^{c_2/\lambda T}\,d\lambda}{(e^{c_2/\lambda T} - 1)^2}\right]\cdot\Delta T$$

$$k_A\Delta A = \left[\frac{1}{\pi D^2}\int_{3.5\,\mu m}^{4.0\,\mu m}\frac{c_1}{\lambda^5}\,\frac{d\lambda}{(e^{c_2/\lambda T} - 1)}\right]\cdot\Delta A$$

$$k_D\Delta D = \left[\frac{-2A}{\pi D^3}\int_{3.5\,\mu m}^{4.0\,\mu m}\frac{c_1}{\lambda^5}\,\frac{d\lambda}{(e^{c_2/\lambda T} - 1)}\right]\cdot\Delta D$$

$$k_\epsilon\Delta\epsilon = \left[\frac{A}{\pi D^2}\int_{3.5\,\mu m}^{4.0\,\mu m}\frac{c_1}{\lambda^5}\,\frac{d\lambda}{(e^{c_2/\lambda T} - 1)}\right]\cdot\Delta\epsilon$$

$$k_\tau\Delta\tau = \left[\frac{A}{\pi D^2}\int_{3.5\,\mu m}^{4.0\,\mu m}\frac{c_1}{\lambda^5}\,\frac{\Delta\tau(\lambda,D)\,d\lambda}{(e^{c_2/\lambda T} - 1)}\right]$$

The error term $\Delta\tau(\lambda,D)$ in the last expression is not explicitly isolated as the others are. It is still possible to use this method to evaluate variance quantitatively, however, by finding the largest and smallest possible values for τ over the range of 3.5 μm to 4.0 μm for the given distance, and using these values to provide a bracketed value range for k_τ based on

$$\Delta\tau_{min} = 1 - \tau_{max}$$

$$\Delta\tau_{max} = 1 - \tau_{min}$$

Numerical Estimation of Reproducibility

The numerical estimation of reproducibility is accomplished by evaluating the coefficients k_T, k_A, k_D, k_ϵ and k_τ for the specified experiment. These coefficient values vary as the values of the defining parameters vary, so that reproducibility is not a constant for a given experimental setup but changes when the unique physical conditions change.

In addition, values for the variances $\sigma^2\Delta T$, $\sigma^2\Delta A$, $\sigma^2\Delta D$, $\sigma^2\Delta\epsilon$, and $\sigma^2\Delta\tau$ must be obtained. This is usually done based on an intimate knowledge of the measurement processes applied to the defining parameters. The smallest scale division on the surveyor's tape used to measure distance, the number of decimal places in the digital temperature readout, and the characteristics of the equipment with which apertures are cut and measured all provide clues to the values of parameter variances.

The coefficient values and the parameter variance values can be inserted in the equation for $\sigma^2\Delta H$ to estimate reproducibility.

While an analytical expression has been developed for the blackbody experiment, several contributing effects have not been treated explicitly, such as alignment and beam strength across the collimated beam. Also, second order and higher terms have been discarded. For an operating aircraft the complete specification of the variance associated with reproducibility would be extremely difficult, if not impossible. However, several terms might be identified which would contain the errors contributing most significantly to variance, and these terms could be quantified.

CONCLUSIONS

UNCERTAINTY OF DATA FROM ONE MEASUREMENT SYSTEM

There are many physical causes for uncertainty among measurement data collected by the same measurement system. For convenience in analyzing and characterizing this uncertainty, these causes may be divided conceptually into three categories:

1. Reproducibility of the experiment
2. Measurement system bias
3. Random distribution of measurement error.

In theory, the reproducibility of the experiment can be quantitatively determined from the defining equation of the experiment and an intimate knowledge of the measurement processes by which the defining parameters for the experiment are evaluated. In

practice, the defining equation or sequence of equations may be difficult to specify completely for complex configurations. Nevertheless, even a partial representation of a complex experiment may be analyzed to quantify the most significant contributors to reproducibility.

Measurement system bias is the most difficult of the three categories to deal with analytically. While no deterministic techniques have been developed, some clues about this bias may be derived from applying a statistical test of significance to measurement data and subsequently performing a qualitative inspection of the data.

The probabilistic distribution of random measurement error is the conceptual area which may be subjected to the most detailed mathematical evaluation. Statistical analysis of the measurement data may be performed to quantify data variability for a range of physical conditions. Numerical analysis may then be applied to characterize data variability as a function of the physical property evaluated by the measurement system.

UNCERTAINTY OF DATA FROM DIFFERENT FACILITIES

The uncertainty which exists among data collected by two different measurement systems includes all the effects described in the preceding section compounded for both facilities. In addition, any discrepancies between the measurement processes used for evaluating the defining parameters at the two facilities, such as bias in measuring the physical conditions, will contribute an additional source of uncertainty.

CHARACTERIZATION OF THE PROBABILISTIC DISTRIBUTION OF MEASUREMENT ERROR

The major goal of this effort is to characterize the probabilistic distribution of measurement error for the Michelson interferometer measurement system. Based on the limited matrix of physical conditions available for this study, a mathematical model

$$\sigma^2 = \rho^2 (H - B)^2 + \sigma_N^2$$

has been suggested to describe the variance of this probabilistic distribution. Here

ρ is a coefficient to be determined by analysis

H is the irradiance due to the source at the collecting optics

B is the mean of the noise distribution

σ_N^2 is the variance of the distribution of noise inherent to the measurement system.

Although insufficient data are available to yield conclusive results, the coefficient ρ appears to be a function of distance. The constant values of ρ, B, and σ_N are characteristic of the particular equipment configuration used for measurement data collection, and must be reevaluated when a measurement system is reconfigured.

PERCENTAGE VARIATION OF MEASUREMENT SAMPLES

The probabilistic distribution of random measurement error is characterized by the standard deviation of the measurement population. For this particular study, the measured parameter is irradiance at the collecting optics of the measurement system. For irradiance values in excess of 1500×10^{-10} watts/cm^2, the standard deviation of any sample of irradiance measurements for the interferometer systems studied in this effort may be estimated from the expected value of irradiance, using the percentage variability factors given in Table 13.

Table 13. Percentage Variability Factors.

Facility	Distance from source, m	Percentage variability (dimensionless)
China Lake	30.48	.24%
	60.96	1.25%
	152.4	1.65%
White Sands	155.0	.7%

To estimate the percentage variability for expected irradiance values closer to the system noise level, the graphs given as Figures 18, 19, 20, and 21 should be used.

RECOMMENDATIONS

UNDERSTANDING THE PROBLEM

As a result of their participation in the test program, personnel interviews, and research of the published reports in the IR community conducted for this effort, the authors have become aware that the problem of data uncertainty is not well understood in IR applications. This same problem has been extensively researched and discussed for other disciplines — in particular for electrical engineering applications. The primary recommendation of this report is that the measurers and users of aircraft IR signature data be made aware

of the nature of the problem. First, an understanding of the causes of measurement data uncertainty would alleviate the political problems resulting from observed discrepancies between results from two different measurement facilities. Second, given the ability to assess the problem, every measurement facility could publish its data with qualifying measurement uncertainty brackets.

Assessment Capability for Measurement Facilities

The recommendation is made that all facilities which measure aircraft IR signatures routinely apply data analysis techniques such as those described in this report to their measurement data. These data analysis algorithms could be implemented as operational computer programs at the facilities so that no additional manpower would be required over present facility staff levels.

Characterizing the Probabilistic Distribution of Measurement Error

When the blackbody experiment reported herein was designed, the nature of the IR measurement uncertainty problem was not completely understood. The experimental design was intended to gather a well-distributed matrix of data for analysis to obtain an understanding of the problem. In fact, the distinction between the reproducibility of the experiment and the probabilistic distribution of measurement error was not recognized. A conceptual division of uncertainty for one measurement system into three categories has been suggested and a mathematical model proposed for describing the probabilistic distribution of measurement error. Well-qualified data should be collected for the sole purpose of verifying or improving this model. This effort should include extensive data in the low signal region to facilitate the analytical determination of system noise. In addition, a sufficiently detailed range of parameter variation should be studied to determine the functional dependence of the irradiance coefficient ρ.* The matrix of data gathered should include a parametric variation over field-of-view values to determine what effect, in any, that factor has on the values of the constants ρ, B, and σ_N in the proposed model. Above all, in any future data collection efforts the editing process at the measurement facilities should be supervised by the data analysts who will be doing the subsequent model verifications.

Studying Other Infrared Measurement Systems

When a verified mathematical model for the characterization of the probabilistic distribution of measurement error for the Michelson interferometer has been accepted, the other commonly used IR measurement systems should be studied. Radiometers and spectrometers are recommended for the next effort. The problems of mathematical characterization of data variability for imaging devices will undoubtedly be much more severe,

*See *Computing Percentage Variability and System Noise.*

and a background of experience of analysis of the more easily described systems should be acquired before attempting to study image data.

Summary

The reader is cautioned that the data variance model proposed in this report has been developed from a relatively small data base, and that additional research may result in modification or replacement of this model. This report is offered as one step in the continuing effort conducted by the JIRS Working Group to improve the quality and usefulness of aircraft IR signature measurement data.

APPENDIX
STATISTICAL DEFINITIONS

For a sample of measurement data containing N items, $\{x_1, x_2, x_3 \ldots, x_N\}$, the Rth moment of the data about a value A is defined as

$$\frac{\sum_{i=1}^{N} (x_i - A)^R}{N}$$

The first moment of the data about the origin (A = 0) is defined as the arithmetic mean $\bar{x}$. This value $\bar{x}$ has the property that the first moment of the data about the arithmetic mean is 0. The second moment of the data about the arithmetic mean determines the sample variance S^2. The square root of this value S is the sample standard deviation, a measure of the dispersion of the data. Formulas for the first four moments for sample data are given in the following chart.

	Moments about *an arbitrary* point A	Moments about *the origin* (A = 0)	Moments about *the arithmetic mean* ($A = \bar{x}$)
First moment	$\frac{\sum_{i=1}^{N} (x_i - A)}{N}$	$\frac{\sum_{i=1}^{N} x_i}{N} = \bar{x}$	$\frac{\sum_{i=1}^{N} (x_i - \bar{x})}{N} = 0$
Second moment	$\frac{\sum_{i=1}^{N} (x_i - A)^2}{N}$	$\frac{\sum_{i=1}^{N} x_i^2}{N}$	$\frac{\sum_{i=1}^{N} (x_i - \bar{x})^2}{N} = \frac{N-1}{N} S^2$
Third moment	$\frac{\sum_{i=1}^{N} (x_i - A)^3}{N}$	$\frac{\sum_{i=1}^{N} x_i^3}{N}$	$\frac{\sum_{i=1}^{N} (x_i - \bar{x})^3}{N} = M_3'$
Fourth moment	$\frac{\sum_{i=1}^{N} (x_i - A)^4}{N}$	$\frac{\sum_{i=1}^{N} x_i^4}{N}$	$\frac{\sum_{i=1}^{N} (x_i - \bar{x})^4}{N} = M_4'$

The moment coefficient of skewness is defined by

$$a_3 = \frac{M_3'}{S^3}$$

For a normal curve, $a_3 = 0$.

The moment coefficient of kurtosis is defined by

$$a_4 = \frac{M_4'}{S^4}$$

For a normal curve, $a_4 = 3$.

JTCG/AS-79-C-003

DISTRIBUTION LIST

Aeronautical Systems Division
Wright-Patterson AFB, OH 45433
Attn: ASD/ENADC (W. Cambron)
Attn: ASD/ENFTV (Lt. R. Berdine)
Attn: ASD/XRE (S. E. Tate)

Air Force Avionics Laboratory
Wright-Patterson AFB, OH 45433
Attn: AFAL/WRW-3 (F. D. Linton)
Attn: AFAL/RWT-4 (L. Meuser)

Air Force Geophysics Laboratory
Hanscom AFB, MA 01730
Attn: (Lt. Col. J. J. Gress)

Air Force Systems Command
Andrews AFB, MD 20334
Attn: AFSC/DLWA (P. L. Sandler)

Air Force Wright Aeronautical Laboratory
AAWA-1
Wright-Patterson AFB, OH 45433
Attn: SAI (D. Powlette)
Attn: AFWAL/FIESD (CDIC) (2 copies)

Applied Technology Laboratory
Army Research and Technology Laboratory
Ft. Eustis, VA 23604
Attn: DAVDL-ATL-ASV (J. D. Ladd)

ARINC Research Corporation
2551 Riva Road
Annapolis, MD 21401
Attn: G. S. Amick

Army Aviation Research and Development Command
P.O. Box 209
St. Louis, MO 63166
Attn: DRCPM-ASE-TM (F. A. Reed)

Army Missile R&D Command
Redstone Arsenal, AL 35809
Attn: DRDMI/TEI (T. Jackson)

Arnold Research Organization
Arnold Engineering Development Center
Arnold AFS, TN 37389
Attn: AEDC/DOT (H. Scott)

Comarco, Inc.
1417 No. Norma
Ridgecrest, CA 93555
Attn: G. Russell (2 copies)

Defense Advanced Research Projects Agency
1400 Wilson Blvd.
Arlington, VA 22209
Attn: DARPA/STO (S. Zakanycz)

Defense Intelligence Agency
Pentagon
Washington, DC 20301
Attn: DC-7B (T. Wee)

Defense Technical Information Center
Cameron Station, Bldg. 5
Alexandria, VA 22314
Attn: DTIC-TCA (12 copies)

Foreign Technology Division (AFSC)
Wright-Patterson AFB, OH 45433
Attn: FTD/SDEO (D. Harruff)

General Dynamics Corporation
P.O. Box 2507
Pomona, CA 91766
Attn: D. W. Blay

General Research Corporation
SWL Division, Suite 700, Park Place
7926 Jones Branch Dr.
McLean, VA 22101
Attn: T. F. King
Attn: R. A. Rollin

National Bureau of Standards
A223 Physics Bldg.
Washington, DC 20234
Attn: F. E. Nicodemus

Naval Air Propulsion Center
P.O. Box 7176
Trenton, NJ 08628
Attn: PE62 (F. Husted)

Naval Air Systems Command
Washington, D. C. 20361
Attn: AIR-5184J (2 copies)
Attn: AIR-5204A (W. Capps)
Attn: AIR-5363F (D. Caldwell)

Naval Air Test Center
Patuxent River, MD 20670
Attn: Code SA83B (D. McCoy)

Naval Intelligence Support Center
4301 Suitland Rd.
Washington, DC 20390
Attn: NISC 42 (P. Roberts)

Naval Metrology Engineering Center
P.O. Box 2505
Pomona, CA 91766
Attn: Code MAG (F. Stimpfle)

Naval Research Laboratory
4555 Overlook Ave., SW
Washington, D. C. 20375
Attn: Code 6533 (J. Dowling)
Attn: Code 6533 (K. Haught)
Attn: Code 1409 (J. M. MacCallum)
Attn: Code 6530-2 (G. L. Stamm)

Naval Surface Weapons Center
Dahlgren Laboratory
Dahlgren, VA 22448
Attn: Code N54 (R. Horman)

Naval Weapon Support Center
Crane, IN 47522
Attn: Code 5042 (C. Dinerman)

Naval Weapons Center
China Lake, CA 93555
Attn: Code 3381 (C. Padgett)
Attn: Code 3912 (E. J. Bevan)
Attn: Code 39403 (J. Wunderlich)
Attn: Code 3943 (J. Socolich)

Nichols Research Corporation
2002 Hogback Rd. Suite 9
Ann Arbor, MI 48104
Attn: J. Mudar

Office of Missile Electronic Warface
White Sands Missile Range, NM 88002
Attn: DELEW-M-TAS (L. H. Holden)

Office of Naval Research
532 South Clark
Chicago, IL 60605
Attn: J. Ivory

Pacific Missile Test Center
Point Mugu, CA 93042
Attn: Code 0160 (J. Francis)
Attn: Code 1232 (D. Stowell)

TEEPA
Eglin AFB, FL 32542
Attn: Dr. H. Register

U. S. Army Electronics Warfare Laboratory
Fort Monmouth, NJ 07703
Attn: DELEW-P (R. G. Pallazzo)

USMC Development Center (D092)
Quantico, VA 22134
Attn: AIR EW DPO (Maj. F. McCaughan)

ABSTRACT CARD

Naval Research Laboratory

Infrared Measurement Variability Analysis, by N. K. Matthis, T. J. Morin, and W. E. Thompson, ARINC Research Corporation. Washington, D.C., NRL, for Joint Technical Coordinating Group/ Aircraft Survivability. September 1980. 68 pp. (JTCG/AS-79-C-003, publication UNCLASSIFIED.)

Two different Michelson Interferometer measurement systems were used to collect spectral radiant intensity data describing blackbody emissions. These data were subjected to statistical and numerical analysis for the purpose of characterizing infrared measurement variability. A mathematical model has been postulated to describe

(Over)
1 card, 8 copies

Naval Research Laboratory

Infrared Measurement Variability Analysis, by N. K. Matthis, T. J. Morin, and W. E. Thompson, ARINC Research Corporation. Washington, D.C., NRL, for Joint Technical Coordinating Group/ Aircraft Survivability. September 1980. 68 pp. (JTCG/AS-79-C-003, publication UNCLASSIFIED.)

Two different Michelson Interferometer measurement systems were used to collect spectral radiant intensity data describing blackbody emissions. These data were subjected to statistical and numerical analysis for the purpose of characterizing infrared measurement variability. A mathematical model has been postulated to describe

(Over)
1 card, 8 copies

Naval Research Laboratory

Infrared Measurement Variability Analysis, by N. K. Matthis, T. J. Morin, and W. E. Thompson, ARINC Research Corporation. Washington, D.C., NRL, for Joint Technical Coordinating Group/ Aircraft Survivability. September 1980. 68 pp. (JTCG/AS-79-C-003, publication UNCLASSIFIED.)

Two different Michelson Interferometer measurement systems were used to collect spectral radiant intensity data describing blackbody emissions. These data were subjected to statistical and numerical analysis for the purpose of characterizing infrared measurement variability. A mathematical model has been postulated to describe

(Over)
1 card, 8 copies

Naval Research Laboratory

Infrared Measurement Variability Analysis, by N. K. Matthis, T. J. Morin, and W. E. Thompson, ARINC Research Corporation. Washington, D.C., NRL, for Joint Technical Coordinating Group/ Aircraft Survivability. September 1980. 68 pp. (JTCG/AS-79-C-003, publication UNCLASSIFIED.)

Two different Michelson Interferometer measurement systems were used to collect spectral radiant intensity data describing blackbody emissions. These data were subjected to statistical and numerical analysis for the purpose of characterizing infrared measurement variability. A mathematical model has been postulated to describe

(Over)
1 card, 8 copies

the variability of infrared measurements based on the results of this analysis. Recommendations are made for future study to verify and extend the results presented in this report.

JTCG/AS-79-C-003

the variability of infrared measurements based on the results of this analysis. Recommendations are made for future study to verify and extend the results presented in this report.

JTCG/AS-79-C-003

the variability of infrared measurements based on the results of this analysis. Recommendations are made for future study to verify and extend the results presented in this report.

JTCG/AS-79-C-003

the variability of infrared measurements based on the results of this analysis. Recommendations are made for future study to verify and extend the results presented in this report.